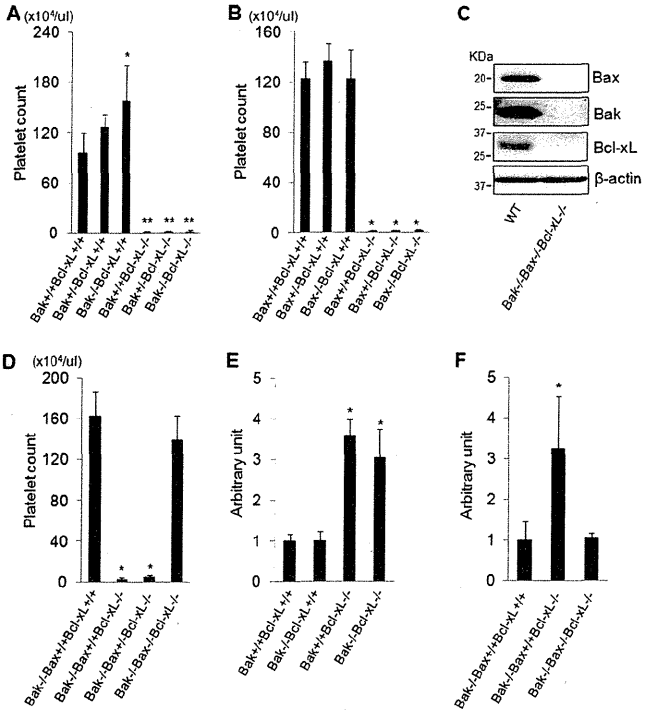

FIGURE 1. **Thrombocytopenia induced by Bcl-xL deficiency is dependent on Bcl-2 effector proteins Bak and Bax.** *Bcl-xL*+/+ and *Bcl-xL*−/− stand for *bcl-x*$^{flox/flox}$ without *pf4-Cre* and *bcl-x*$^{flox/flox}$ with *pf4-Cre*, respectively. *Bak*+/+, *Bak*+/−, and *Bak*−/− stand for *bak*$^{+/+}$, *bak*$^{+/-}$, and *bak*$^{-/-}$, respectively. *WT* stands for wild type. *A*, platelet counts of the offspring from mating of *bak*$^{+/-}$*bcl-x*$^{flox/flox}$ *pf4-Cre* mice and *bak*$^{+/-}$*bcl-x*$^{flox/flox}$ mice (more than four mice per group; *, $p < 0.01$ *versus* all other groups; **, $p < 0.01$ *versus* Bcl-xL+/+ groups). *B*, platelet counts of the offspring from mating of *bax*$^{+/-}$*bcl-x*$^{flox/flox}$ *pf4-Cre* mice and *bax*$^{+/-}$*bcl-x*$^{flox/flox}$ mice (more than five mice per group; *, $p < 0.01$ *versus* Bcl-xL+/+ groups). *Bax*+/+, *Bax*+/−, and *Bax*−/− stand for *bax*$^{+/+}$, *bax*$^{+/-}$, and *bax*$^{-/-}$, respectively. *C*, Western blot of platelet lysates for the expression of Bcl-xL, Bak, and Bax. *D*, platelet counts of the offspring from mating of *bak*$^{-/-}$*bax*$^{flox/+}$*bcl-x*$^{flox/flox}$ *pf4-Cre* mice and *bak*$^{-/-}$*bax*$^{flox/+}$*bcl-x*$^{flox/flox}$ mice (more than eight mice per group; *, $p < 0.01$ *versus* Bak−/−Bax+/+Bcl-xL+/+ group and Bak−/−Bax−/−Bcl-xL−/− group. *Bax*+/+, *Bax*+/−, and *Bax*−/− stand for *bax*$^{+/+}$, *bax*$^{flox/+}$ with *pf4-Cre*, and *bax*$^{flox/flox}$ with *pf4-Cre*, respectively. *E*, serum caspase-3/7 activity of the offspring from mating of *bak*$^{+/-}$*bcl-x*$^{flox/flox}$ *pf4-Cre* mice and *bak*$^{+/-}$*bcl-x*$^{flox/flox}$ mice (n = 5 or 6/group; *, $p < 0.01$ *versus* Bcl-xL+/+ group). *F*, serum caspase-3/7 activity of the offspring from mating of *bak*$^{-/-}$*bax*$^{flox/+}$*bcl-x*$^{flox/flox}$ *pf4-Cre* mice and *bak*$^{-/-}$*bax*$^{flox/+}$*bcl-x*$^{flox/flox}$ mice (n = 8/group; *, $p < 0.01$ *versus* all). *Bax*+/+, *Bax*+/−, and *Bax*−/− stand for *bax*$^{+/+}$, *bax*$^{flox/+}$ with *pf4-Cre*, and *bax*$^{flox/flox}$ with *pf4-Cre*, respectively.

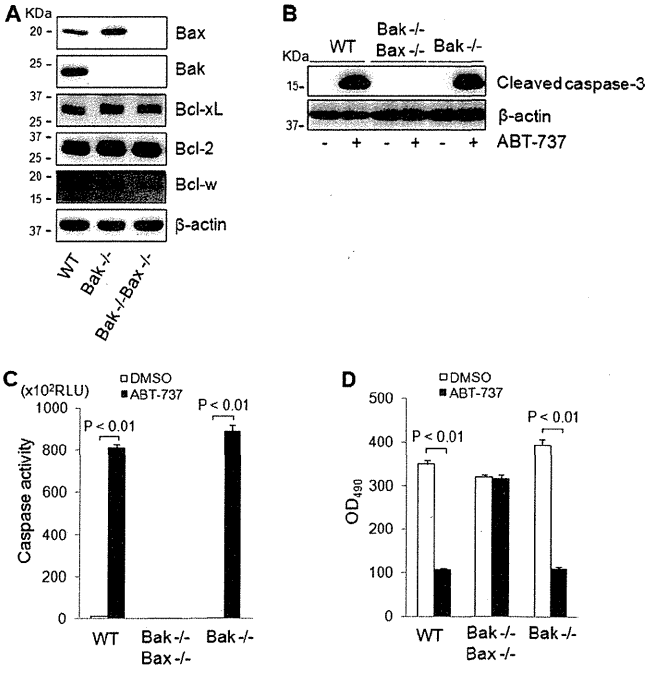

FIGURE 2. **ABT-737 treatment provokes Bak/Bax-dependent apoptosis in platelets.** *WT*, *Bak*−/−*Bax*−/−, and *Bak*−/− stand for wild type, *bak*−/−*bax*$^{flox/flox}$ with *pf4-Cre*, and *bak*−/−, respectively. *A*, Western blot of platelet lysates for the expression of Bak, Bax, Bcl-xL, Bcl-2, and Bcl-w. *B*, platelets (3.0×10^7) were incubated with 10 μM ABT-737 or vehicle for 2 h at room temperature. A Western blot of platelet lysates for the expression of cleaved caspase-3 is shown. *C* and *D*, platelets (2.0×10^6) were incubated with 10 μM ABT-737 or vehicle for 2 h at room temperature. *C*, caspase-3/7 activity of platelet supernatant (n = 4/group). *D*, MTS assay (n = 5/group). *RLU*, relative light units.

phobic groove of these proteins (31). Western blot revealed that these antiapoptotic Bcl-2 proteins existed in platelets (Fig. 2*A*), and ABT-737 has already been reported to cause apoptosis in platelets in both *in vivo* and *in vitro* settings (7, 8). We first examined whether ABT-737-induced platelet apoptosis was executed via the Bak/Bax-dependent mitochondrial pathway. In platelets isolated from wild-type mice, administration of ABT-737 caused cleavage of caspase-3 (Fig. 2*B*). Supernatants of ABT-737-treated platelets showed marked elevation of caspase-3/7 activity (Fig. 2*C*). In addition, platelet cellular viability, which can be assessed by MTS assay (3, 4), decreased upon ABT-737 treatment (Fig. 2*D*). On the other hand, although expression of targeted antiapoptotic Bcl-2 proteins was not different between platelets from wild-type mice and Bak/Bax double knock-out mice (Fig. 2*A*), ABT-737 treatment neither caused caspase activation nor impaired cellular integrity in Bak/Bax-deficient platelets (Fig. 2, *B–D*). These findings demonstrated that ABT-737 caused platelet apoptosis via the Bak/Bax-dependent mitochondrial pathway. Interestingly, unlike what was reported previously (8), Bak deficiency could alleviate neither caspase activation nor loss of cellular viability in ABT-737-treated platelets (Fig. 2, *B–D*), offering evidence of the redundancy of Bak and Bax proteins in executing apoptosis in platelets under inhibition of these antiapoptotic Bcl-2 proteins.

ABT-737 Treatment Causes Bax Activation in Platelets—After ABT-737 treatment of the platelets, we next examined the activation status of the Bax protein in these platelets. In general, Bax activation is divided into sequential steps. When subjected to a variety of apoptotic stimuli, the Bax protein first undergoes a conformational change such as exposure of the amino terminus. This active form is translocated from the cytosol to the mitochondria. Finally, mitochondrial Bax undergoes self-oligomerization, leading to permeabilization of the outer mitochondrial membrane (32). We found that upon addition of ABT-737 to platelets the Bax protein underwent a conformational change as demonstrated by Western blotting upon immunoprecipitation with an antibody that specifically recognizes the amino terminus of the Bax protein (33) (Fig. 3*A*). In addition, upon ABT-737 treatment, the Bax protein was translocated from the cytosol to the mitochondria (Fig. 3*B*) and then underwent homo-oligomerization (Fig. 3*C*). These findings indicated that inhibition of antiapoptotic Bcl-2 proteins in

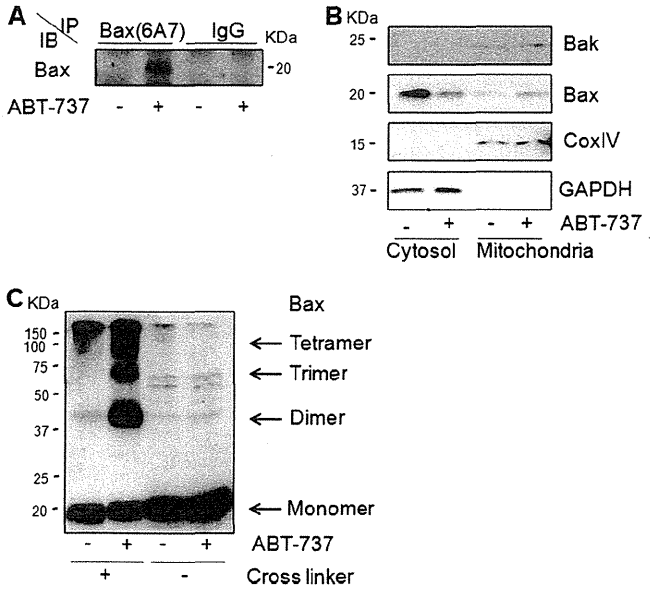

FIGURE 3. **ABT-737 treatment causes Bax activation in platelets.** *A–C*, platelets (1.0×10^8) isolated from C57BL/6J mice were incubated with 10 μM ABT-737 or vehicle for 2 h at room temperature. *A*, Western blot of platelet lysates for the expression of Bax after immunoprecipitation (*IP*) using mouse antibody that specifically recognizes activated Bax (6A7) or mouse control IgG (active Bax exposes an amino-terminal epitope (amino acids 12–24) that is recognized by 6A7). *B*, Western blot for the expression of Bak, Bax, *CoxIV* (cytochrome c oxidase IV), and GAPDH after cellular fractionation of the platelet lysates. *C*, Western blot for the expression of Bax after incubation of the platelet lysates with or without protein cross-linkers (5 mM bismaleimidohexane and 5 mM bis(sulfosuccinimidyl) suberate). *IB*, immunoblot.

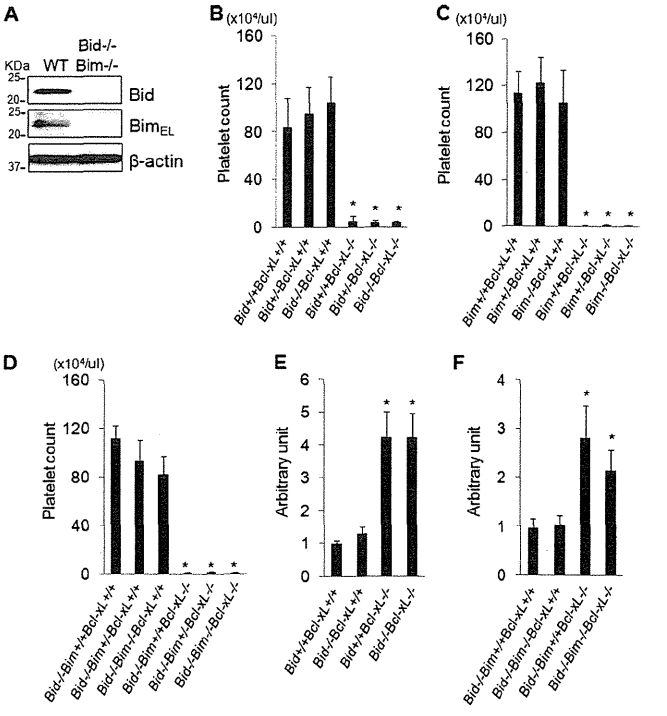

FIGURE 4. **Thrombocytopenia induced by Bcl-xL deficiency does not require BH3-only activator proteins Bid and Bim.** *Bcl-xL+/+* and *Bcl-xL−/−* stand for *bcl-x$^{flox/flox}$* without *pf4-Cre* and *bcl-x$^{flox/flox}$* with *pf4-Cre*, respectively. *Bid+/+*, *Bid+/−*, and *Bid−/−* stand for *bid$^{+/+}$*, *bid$^{+/-}$*, and *bid$^{-/-}$*, respectively. *Bim+/+*, *Bim+/−*, and *Bim−/−* stand for *bim$^{+/+}$*, *bim$^{+/-}$*, and *bim$^{-/-}$*, respectively. *WT* and *Bid−/−Bim−/−* stand for wild type and *bid$^{-/-}$bim$^{-/-}$*, respectively. *A*, Western blot of platelet lysates for the expression of Bid and Bim$_{EL}$. *B*, platelet counts of the offspring from mating of *bid$^{+/-}$bcl-x$^{flox/flox}$ pf4-Cre* mice and *bid$^{+/-}$bcl-x$^{flox/flox}$* mice (more than five mice per group; *, $p < 0.01$ *versus* Bcl-xL+/+ groups). *C*, platelet counts of the offspring from mating of *bim$^{+/-}$bcl-x$^{flox/flox}$ pf4-Cre* mice and *bim$^{+/-}$bcl-x$^{flox/flox}$* mice (more than seven mice per group; *, $p < 0.01$ *versus* Bcl-xL+/+ groups). *D*, platelet counts of the offspring from mating of *bid$^{-/-}$bim$^{+/-}$bcl-x$^{flox/flox}$ pf4-Cre* mice and *bid$^{-/-}$bim$^{+/-}$bcl-x$^{flox/flox}$* mice (more than five mice per group; *, $p < 0.01$ *versus* Bcl-xL+/+ groups). *E*, serum caspase-3/7 activity of the offspring from mating of *bid$^{+/-}$bcl-x$^{flox/flox}$ pf4-Cre* mice and *bid$^{+/-}$bcl-x$^{flox/flox}$* mice ($n = 4-6$/group; *, $p < 0.01$ *versus* Bcl-xL+/+ groups). *F*, serum caspase-3/7 activity of the offspring from mating of *bid$^{-/-}$bim$^{+/-}$bcl-x$^{flox/flox}$ pf4-Cre* mice and *bid$^{-/-}$bim$^{+/-}$bcl-x$^{flox/flox}$* mice ($n = 4-6$/group; *, $p < 0.01$ *versus* Bcl-xL+/+ groups).

platelets caused Bax activation, promoting Bak/Bax-dependent mitochondrial apoptosis followed by caspase activation.

Thrombocytopenia Induced by Bcl-xL Deficiency Does Not Require BH3-only Activator Proteins Bid and Bim—We explored whether Bak/Bax-dependent platelet apoptosis induced by Bcl-xL deficiency requires the direct activator proteins Bid and Bim. Western blot revealed that Bid and Bim were both present in platelets (Fig. 4*A*). We generated Bcl-xL/Bid double knock-out mice and Bcl-xL/Bim double knock-out mice by mating thrombocyte-specific Bcl-xL knock-out mice with systemic Bid knock-out mice or Bim knock-out mice, respectively. These double knock-out mice showed massive thrombocytopenia that was not alleviated at all compared with that of thrombocyte-specific Bcl-xL knock-out mice (Fig. 4, *B* and *C*). It was possible that, in Bcl-xL-deficient platelets, the existence of either Bid or Bim was sufficient to activate Bak/Bax directly, leading to platelet apoptosis in these double knock-out mice. We then generated Bcl-xL, Bid, and Bim triple knock-out mice by mating Bcl-xL/Bid double knock-out mice with Bcl-xL/Bim double knock-out mice. These triple knock-out mice still showed massive thrombocytopenia without any difference of platelet count compared with that of Bcl-xL/Bid double knock-out mice (Fig. 4*D*). These findings clearly demonstrated that BH3-only activator proteins Bid and Bim were dispensable for the severe thrombocytopenia induced by thrombocyte-specific Bcl-xL deletion *in vivo*. In addition, caspase activation in thrombocyte-specific Bcl-xL knock-out mice was not alleviated even in the Bid and Bim double knock-out background (Fig. 4, *E* and *F*), suggesting that the lack of Bcl-xL required neither Bid nor Bim to trigger Bak/Bax-dependent platelet apoptosis.

Bax Activation and Subsequent Apoptotic Cell Death Provoked by ABT-737 Can Proceed in Absence of Bid and Bim—To investigate whether Bax can be activated by inhibition of anti-apoptotic Bcl-2 proteins even in the absence of Bid and Bim, we isolated platelets from Bid and Bim double knock-out mice. A Western blot study confirmed that neither Bid nor Bim existed in platelets of the double knock-out mice (Fig. 4*A*) and showed that Puma protein, another putative direct activator (13), was not detected in platelets of either wild-type mice or Bid/Bim double knock-out mice (Fig. 5*A*). The expression of antiapoptotic Bcl-2 proteins including Bcl-xL, Bcl-2, and Bcl-w was unchanged between these mice (Fig. 5*A*). Upon ABT-737 treatment, the Bax protein in Bid/Bim-deficient platelets could undergo conformational change (Fig. 5*B*), translocation from the cytosol to the mitochondria (Fig. 5*C*), and homo-oligomerization (Fig. 5*D*). These results clearly demonstrated that ABT-

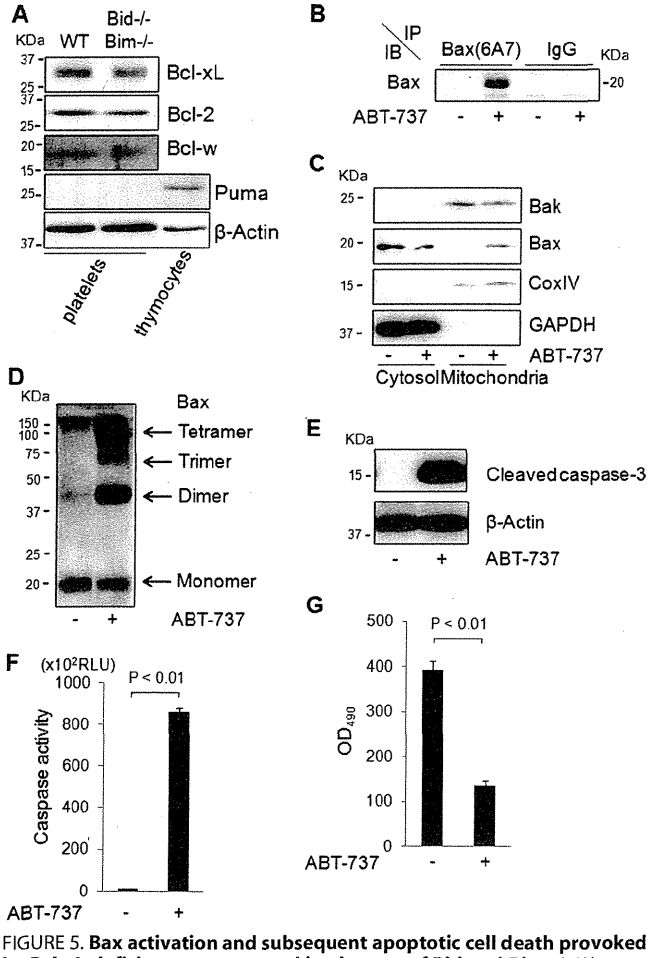

FIGURE 5. **Bax activation and subsequent apoptotic cell death provoked by Bcl-xL deficiency can proceed in absence of Bid and Bim.** *A*, Western blot of platelet lysates for the expression of Puma, Bcl-2, Bcl-w, and Bcl-xL. *WT* and *Bid−/−Bim−/−* stand for wild type and $bid^{-/-}bim^{-/-}$, respectively. *B–E*, platelets (1.0×10^8) isolated from Bid/Bim double knock-out mice were incubated with 10 μM ABT-737 or vehicle for 2 h at room temperature. *B*, Western blot for the expression of Bax after immunoprecipitation (*IP*) using mouse antibody that specifically recognizes activated Bax (6A7) or mouse control IgG. *C*, Western blot for the expression of Bak, Bax, *CoxIV* (cytochrome c oxidase IV), and GAPDH after cellular fractionation of the platelet lysates. *D*, Western blot for the expression of Bax after incubation of the platelet lysates with protein cross-linkers (5 mM bismaleimidohexane and 5 mM bis(sulfosuccinimidyl) suberate). *E*, Western blot of platelet lysates for the expression of cleaved caspase-3. *F* and *G*, platelets (2.0×10^6) isolated from Bid/Bim double knock-out mice were incubated with 10 μM ABT-737 or vehicle for 2 h at room temperature. *F*, caspase-3/7 activity of platelet supernatant ($n = 4$/group). *G*, MTS assay ($n = 5$/group). *IB*, immunoblot; *RLU*, relative light units.

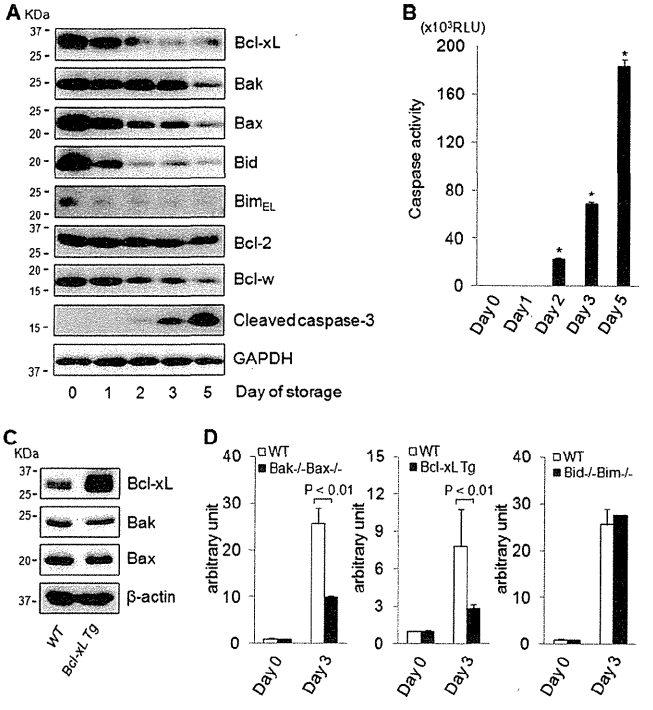

FIGURE 6. **Spontaneous apoptotic cell death in stored platelets occurs with decline of Bcl-xL despite decrease in Bid and Bim.** *A* and *B*, platelet-rich plasma derived from a healthy volunteer was stored for the indicated time course. *A*, Western blot of stored platelet lysates for the expression of Bcl-xL, Bak, Bax, Bid, Bim_{EL}, Bcl-w, Bcl-2, cleaved caspase-3, and GAPDH. Equal numbers of platelets were loaded per sample. *B*, caspase-3/7 activity of supernatant derived from platelet-rich plasma ($n = 4$/group; *, $p < 0.01$ *versus* all other groups). *C*, Western blot of platelet lysates derived from Bcl-xL transgenic mice for the expression of Bcl-xL, Bak, and Bax. *WT* and *Bcl-xL Tg* stand for wild-type mice and Bcl-xL transgenic mice, respectively. *D*, platelets derived from C57BL/6J mice, Bak/Bax double knock-out mice, Bcl-xL transgenic mice, and Bid/Bim double knock-out mice were stored for the indicated time course. Caspase-3/7 activity of stored platelet supernatant was assessed and is presented as the -fold induction compared with freshly isolated platelet supernatant ($n = 4$/group). *WT*, *Bak−/−Bax−/−*, and *Bid−/−Bim−/−* stand for wild-type, $bak^{-/-}bax^{flox/flox}$ with *pf4-Cre*, and $bid^{-/-}bim^{-/-}$ mice, respectively. *Bcl-xL Tg* stands for Bcl-xL transgenic mice. *RLU*, relative light units.

737-induced Bax activation did not require the direct activator proteins Bid and Bim. Upon ABT-737 treatment of Bid/Bim-deficient platelets, cleavage of caspase-3 and elevation of caspase-3/7 activity were both observed (Fig. 5, *E* and *F*), and the MTS assay demonstrated that platelet cellular viability was also impaired (Fig. 5*G*). These findings indicated that Bid and Bim were dispensable for Bak/Bax-dependent platelet apoptosis provoked by inhibition of antiapoptotic Bcl-2 proteins.

Spontaneous Apoptotic Cell Death in Stored Human Platelets Occurs with Decline of Bcl-xL Despite Decrease in Bid and Bim—In stored human platelets, phosphatidylserine exposure increases with caspase-3 activation (4, 5), which leads to spontaneous platelet apoptosis, but the exact molecular mechanism of this process remains elusive. This led us to examine the profile of Bcl-2 family proteins in human platelets during the course of storage. In stored platelets, cleaved caspase-3 gradually increased (Fig. 6*A*) and caspase-3/7 activity rose simultaneously (Fig. 6*B*), indicating that the platelets steadily underwent apoptotic cell death with storage time. Regarding the Bcl-2 family protein profile, although expression of Bcl-xL and Bax proteins gradually decreased with time, the decrease in Bak expression occurred at a later time point (Fig. 6*A*). As for BH3-only direct activator proteins, Bid and Bim expression also decreased with time (Fig. 6*A*). To examine the involvement of Bcl-2 family proteins in spontaneous apoptosis in stored platelets, caspase-3/7 activity was measured in platelets from wild-type mice, Bak/Bax double knock-out mice, Bcl-xL transgenic mice, and Bid/Bim double knock-out mice upon storage. A Western blot revealed that Bcl-xL protein increased in platelets isolated from Bcl-xL transgenic mice compared with wild-type mice, whereas expression of effector proteins Bak and Bax did not differ between them (Fig. 6*C*). Although wild-type platelets showed elevation of the caspase-3/7 activity upon storage, it was significantly lower in Bak/Bax-deficient platelets than in

wild-type platelets (Fig. 6*D*). These findings indicated that Bak/Bax-dependent mitochondrial apoptosis played an important role in the execution of spontaneous apoptosis in stored platelets. Furthermore, caspase activation was alleviated in Bcl-xL-overexpressing platelets compared with wild-type platelets upon storage (Fig. 6*D*), suggesting an antiapoptotic function of Bcl-xL in stored platelets. On the other hand, caspase-3/7 activity increased in Bid/Bim-deficient platelets and was not different from that in wild-type platelets (Fig. 6*D*), suggesting that direct activator proteins Bid and Bim are dispensable for the spontaneous platelet apoptosis upon storage.

DISCUSSION

In the mitochondrial pathway, apoptotic cell death is dependent on activation of the proapoptotic effector proteins Bak and Bax. Cells lacking both Bak and Bax are resistant to multiple apoptotic stimuli (34). Genetic studies have revealed that Bax or Bak single knock-out mice have less pronounced phenotypes compared with Bak/Bax double knock-out mice, which display various severe defects during development, indicating the redundancy of their involvement in apoptosis (30, 35). With regard to the mitochondrial apoptosis machinery in platelets, the involvement of Bax seemed to be less critical because platelet numbers in Bax knock-out mice were normal in contrast to the thrombocytosis displayed in Bak knock-out mice (30, 35). However, our *in vitro* study revealed that ABT-737 could provoke apoptosis even in Bak-deficient platelets. Moreover, our *in vivo* studies have clearly demonstrated that either Bax or Bak was sufficient to cause platelet apoptosis in the absence of Bcl-xL, indicating that Bax and Bak are redundant and equivalently important for the mitochondrial apoptosis in platelets.

In support of the displacement model, co-immunoprecipitation studies revealed complexes of Bak with a variety of antiapoptotic proteins (36). However, the major concern with this model is that Bax is presumed to exist mainly in a cytosolic fraction as a monomer (37). Thus, Bax activation might not be controlled by displacement (38). Unlike Bak activation, sequential steps are necessary for Bax activation such as a conformational change, mitochondrial translocation, and homo-oligomerization. Recent reports have revealed the mechanism of how activator proteins Bid and Bim are directly involved in these steps and initiate Bax activation (39, 40). In the present study, we showed that all the serial steps of Bax activation can adequately proceed without the involvement of the activator proteins Bid and Bim *in vitro*. Moreover, Bak/Bax-dependent mitochondrial apoptosis could be fully executed by inhibition of antiapoptotic Bcl-2-like proteins even if the direct activator proteins Bid and Bim did not exist. Similar results have been presented by Willis *et al.* (15), who showed that embryonic fibroblasts from Bid and Bim double knock-out, when infected with retrovirus expressing BH3 sensitizer proteins, could undergo apoptosis *in vitro*. Based on their results, they claimed that the Bax protein may be constitutively active and inhibited through binding to antiapoptotic Bcl-2-like proteins for cells to survive. However, in our *in vitro* study, we could not detect physiological interaction between Bax and Bcl-xL in platelets. Therefore, it is difficult to evaluate whether Bak and/or Bax is active or inactive at the default state in platelets. On the other hand, genetically modified mice clearly showed that retrieval of direct activator proteins could not prevent caspase activation and thrombocytopenia induced by the lack of Bcl-xL. These findings demonstrated, for the first time, *in vivo* evidence that direct activator proteins Bid and Bim were dispensable for apoptosis execution provoked by the loss of antiapoptotic Bcl-2-family proteins.

Because ABT-737 can bind to and neutralize Bcl-2, Bcl-w, and Bcl-xL, all of which are present in platelets (Figs. 2*A* and 6*A*), it is difficult to directly conclude that the *in vitro* results from our ABT-737 study exactly reflect our *in vivo* results obtained from Bcl-xL deletion. However, in addition to reports that neither systemic Bcl-w knock-out nor Bcl-2 knock-out mice exhibit any phenotypes with respect to platelet counts (41–43), our *in vivo* results of massive thrombocytopenia seen in thrombocyte-specific Bcl-xL knock-out mice indicated that the antiapoptotic role of Bcl-2 and Bcl-w in platelets was apparently less important than that of Bcl-xL. Even if Bcl-2 and Bcl-w were involved in our *in vitro* results, our present results clearly demonstrated that neither Bid nor Bim is required for Bax activation and following mitochondrial apoptosis by inhibition of antiapoptotic Bcl-2 family proteins. Regarding the other antiapoptotic members of the Bcl-2 family, systemic A1a knock-out mice were not reported with any phenotype with respect to platelet counts (44). Mcl-1 is a rapid turnover protein and could not be detected in platelets (supplemental Fig. 1). Therefore, Bcl-xL may be the main antiapoptotic Bcl-2 family protein with functional significance in platelets. This simplicity may explain why Bid and Bim deficiency failed to ameliorate the phenotype of Bcl-xL knock-out in platelets in contrast to other scenarios in which Bid or Bim is apparently indispensable (19–21). Fatal polycystic kidney disease and lymphopenia observed in Bcl-2 knock-out mice are ameliorated in a Bim knock-out background (19). In this case, lymphocytes and other cell lineages may possess Bcl-2 and other antiapoptotic Bcl-2 proteins such as Mcl-1 (45). Hepatocyte apoptosis observed in hepatocyte-specific knock-out of Mcl-1 or Bcl-xL is ameliorated in a Bid knock-out background (20, 21). In this case, hepatocytes clearly have two critical antiapoptotic Bcl-2 family proteins, Bcl-xL and Mcl-1, and Bid may switch binding partners from one to the other in the case of deficiency of either protein. Bid and Bim could regulate the rheostat balance between antiapoptotic and proapoptotic Bcl-2 family proteins, which may become irrelevant if none of the antiapoptotic Bcl-2 family proteins are present.

Although among the BH3-only proteins Bid and Bim are recognized as the putative direct activators, Puma, one of the other BH3-only proteins, has been reported to have the ability to interact directly with effector proteins (13). However, a recent report has pointed out that Puma is a sensitizer protein, which indirectly activates Bak or Bax (46). Hence, its actual mechanism of action in apoptosis remains obscure and disputed. Importantly, in contrast to thymocyte tissue, a Western blot did not show a detectable amount of Puma protein in platelets (Fig. 5*A*), indicating that it might not be involved in the platelet apoptosis machinery. However, we could not exclude the possibility that other proteins may function as alternative direct acti-

vators in the absence of Bid and Bim, leading to Bax activation and mitochondrial apoptosis in platelets upon inactivation of antiapoptotic Bcl-2 family proteins.

In stored platelets, because of the lack of *de novo* protein synthesis, each protein may gradually decrease in relation to its half-life. Our current results showed that the decline of Bcl-xL and Bax protein was much faster than that of Bak protein, and the disruption of the balance between anti- and proapoptotic multidomain Bcl-2 proteins seemed to be associated with apoptosis in stored human platelets. In fact, upon storage, caspase activation was weakened in Bak/Bax-deficient or Bcl-xL-overexpressing platelets compared with wild-type platelets. Taken together with these findings, the balance between anti- and proapoptotic multidomain Bcl-2 family proteins seems to dictate the cellular fate of the life and death of stored platelets. Similar degradation of the Bcl-2 family proteins should occur in circulation, which may explain why Bak knock-out mice displayed mild thrombocytosis *in vivo* (Fig. 1*A*). On the other hand, spontaneous apoptosis occurred in stored platelets despite the absence of activator proteins Bid and Bim. Although in most physiological contexts cellular death is an active decision made by regulating BH3-only proteins, our present findings suggest that activator proteins Bid and Bim were dispensable for Bak/Bax-dependent spontaneous apoptosis in stored platelets.

How anti- and proapoptotic Bcl-2 family proteins interact to maintain cellular integrity and to command cellular survival and death is one of the most important issues that remain to be clearly determined. Although their networks seem to vary depending on the cellular context, our present findings provide an *in vivo* example indicating that the absence of antiapoptotic Bcl-2-like proteins can induce activation of the effector protein Bax, leading to apoptosis without the involvement of the activator proteins Bid and Bim.

Acknowledgments—We sincerely thank Radek Skoda (University Hospital Basel) and Lothar Hennighausen (National Institutes of Health) for providing the pf4-Cre mice and floxed bcl-x mice, respectively. We also thank Abbott Laboratories for providing ABT-737.

REFERENCES

1. Holmsen, H. (1989) *Ann. Med.* **21,** 23–30
2. Ault, K. A., and Knowles, C. (1995) *Exp. Hematol.* **23,** 996–1001
3. Bertino, A. M., Qi, X. Q., Li, J., Xia, Y., and Kuter, D. J. (2003) *Transfusion* **43,** 857–866
4. Li, J., Xia, Y., Bertino, A. M., Coburn, J. P., and Kuter, D. J. (2000) *Transfusion* **40,** 1320–1329
5. Perrotta, P. L., Perrotta, C. L., and Snyder, E. L. (2003) *Transfusion* **43,** 526–535
6. Vanags, D. M., Orrenius, S., and Aguilar-Santelises, M. (1997) *Br. J. Haematol.* **99,** 824–831
7. Zhang, H., Nimmer, P. M., Tahir, S. K., Chen, J., Fryer, R. M., Hahn, K. R., Iciek, L. A., Morgan, S. J., Nasarre, M. C., Nelson, R., Preusser, L. C., Reinhart, G. A., Smith, M. L., Rosenberg, S. H., Elmore, S. W., and Tse, C. (2007) *Cell Death Differ.* **14,** 943–951
8. Mason, K. D., Carpinelli, M. R., Fletcher, J. I., Collinge, J. E., Hilton, A. A., Ellis, S., Kelly, P. N., Ekert, P. G., Metcalf, D., Roberts, A. W., Huang, D. C., and Kile, B. T. (2007) *Cell* **128,** 1173–1186
9. Kodama, T., Takehara, T., Hikita, H., Shimizu, S., Li, W., Miyagi, T., Hosui, A., Tatsumi, T., Ishida, H., Tadokoro, S., Ido, A., Tsubouchi, H., and Hayashi, N. (2010) *Gastroenterology* **138,** 2487–2498
10. Chipuk, J. E., and Green, D. R. (2008) *Trends Cell Biol.* **18,** 157–164
11. Adams, J. M., and Cory, S. (2007) *Curr. Opin. Immunol.* **19,** 488–496
12. Leber, B., Lin, J., and Andrews, D. W. (2010) *Oncogene* **29,** 5221–5230
13. Kim, H., Rafiuddin-Shah, M., Tu, H. C., Jeffers, J. R., Zambetti, G. P., Hsieh, J. J., and Cheng, E. H. (2006) *Nat. Cell Biol.* **8,** 1348–1358
14. Willis, S. N., and Adams, J. M. (2005) *Curr. Opin. Cell Biol.* **17,** 617–625
15. Willis, S. N., Fletcher, J. I., Kaufmann, T., van Delft, M. F., Chen, L., Czabotar, P. E., Ierino, H., Lee, E. F., Fairlie, W. D., Bouillet, P., Strasser, A., Kluck, R. M., Adams, J. M., and Huang, D. C. (2007) *Science* **315,** 856–859
16. Kuwana, T., Bouchier-Hayes, L., Chipuk, J. E., Bonzon, C., Sullivan, B. A., Green, D. R., and Newmeyer, D. D. (2005) *Mol. Cell* **17,** 525–535
17. Letai, A., Bassik, M. C., Walensky, L. D., Sorcinelli, M. D., Weiler, S., and Korsmeyer, S. J. (2002) *Cancer Cell* **2,** 183–192
18. Billen, L. P., Kokoski, C. L., Lovell, J. F., Leber, B., and Andrews, D. W. (2008) *PLoS Biol.* **6,** e147
19. Bouillet, P., Cory, S., Zhang, L. C., Strasser, A., and Adams, J. M. (2001) *Dev. Cell* **1,** 645–653
20. Hikita, H., Takehara, T., Kodama, T., Shimizu, S., Hosui, A., Miyagi, T., Tatsumi, T., Ishida, H., Ohkawa, K., Li, W., Kanto, T., Hiramatsu, N., Hennighausen, L., Yin, X. M., and Hayashi, N. (2009) *Hepatology* **50,** 1972–1980
21. Hikita, H., Takehara, T., Shimizu, S., Kodama, T., Li, W., Miyagi, T., Hosui, A., Ishida, H., Ohkawa, K., Kanto, T., Hiramatsu, N., Yin, X. M., Hennighausen, L., Tatsumi, T., and Hayashi, N. (2009) *Hepatology* **50,** 1217–1226
22. Takehara, T., Tatsumi, T., Suzuki, T., Rucker, E. B., 3rd, Hennighausen, L., Jinushi, M., Miyagi, T., Kanazawa, Y., and Hayashi, N. (2004) *Gastroenterology* **127,** 1189–1197
23. Tiedt, R., Schomber, T., Hao-Shen, H., and Skoda, R. C. (2007) *Blood* **109,** 1503–1506
24. Yin, X. M., Wang, K., Gross, A., Zhao, Y., Zinkel, S., Klocke, B., Roth, K. A., and Korsmeyer, S. J. (1999) *Nature* **400,** 886–891
25. Gordon, J. W., Scangos, G. A., Plotkin, D. J., Barbosa, J. A., and Ruddle, F. H. (1980) *Proc. Natl. Acad. Sci. U.S.A.* **77,** 7380–7384
26. Takehara, T., and Takahashi, H. (2003) *Cancer Res.* **63,** 3054–3057
27. Feinstein, M. B., and Fraser, C. (1975) *J. Gen. Physiol.* **66,** 561–581
28. Chaiyarit, S., and Thongboonkerd, V. (2009) *Anal. Biochem.* **394,** 249–258
29. Yamagata, H., Shimizu, S., Nishida, Y., Watanabe, Y., Craigen, W. J., and Tsujimoto, Y. (2009) *Oncogene* **28,** 3563–3572
30. Lindsten, T., Ross, A. J., King, A., Zong, W. X., Rathmell, J. C., Shiels, H. A., Ulrich, E., Waymire, K. G., Mahar, P., Frauwirth, K., Chen, Y., Wei, M., Eng, V. M., Adelman, D. M., Simon, M. C., Ma, A., Golden, J. A., Evan, G., Korsmeyer, S. J., MacGregor, G. R., and Thompson, C. B. (2000) *Mol. Cell* **6,** 1389–1399
31. Oltersdorf, T., Elmore, S. W., Shoemaker, A. R., Armstrong, R. C., Augeri, D. J., Belli, B. A., Bruncko, M., Deckwerth, T. L., Dinges, J., Hajduk, P. J., Joseph, M. K., Kitada, S., Korsmeyer, S. J., Kunzer, A. R., Letai, A., Li, C., Mitten, M. J., Nettesheim, D. G., Ng, S., Nimmer, P. M., O'Connor, J. M., Oleksijew, A., Petros, A. M., Reed, J. C., Shen, W., Tahir, S. K., Thompson, C. B., Tomaselli, K. J., Wang, B., Wendt, M. D., Zhang, H., Fesik, S. W., and Rosenberg, S. H. (2005) *Nature* **435,** 677–681
32. Chipuk, J. E., Moldoveanu, T., Llambi, F., Parsons, M. J., and Green, D. R. (2010) *Mol. Cell* **37,** 299–310
33. Hsu, Y. T., and Youle, R. J. (1997) *J. Biol. Chem.* **272,** 13829–13834
34. Wei, M. C., Zong, W. X., Cheng, E. H., Lindsten, T., Panoutsakopoulou, V., Ross, A. J., Roth, K. A., MacGregor, G. R., Thompson, C. B., and Korsmeyer, S. J. (2001) *Science* **292,** 727–730
35. Knudson, C. M., Tung, K. S., Tourtellotte, W. G., Brown, G. A., and Korsmeyer, S. J. (1995) *Science* **270,** 96–99
36. Willis, S. N., Chen, L., Dewson, G., Wei, A., Naik, E., Fletcher, J. I., Adams, J. M., and Huang, D. C. (2005) *Genes Dev.* **19,** 1294–1305
37. Antonsson, B., Montessuit, S., Sanchez, B., and Martinou, J. C. (2001) *J. Biol. Chem.* **276,** 11615–11623
38. Leber, B., Lin, J., and Andrews, D. W. (2007) *Apoptosis* **12,** 897–911
39. Gavathiotis, E., Suzuki, M., Davis, M. L., Pitter, K., Bird, G. H., Katz, S. G., Tu, H. C., Kim, H., Cheng, E. H., Tjandra, N., and Walensky, L. D. (2008)

Nature **455,** 1076–1081
40. Lovell, J. F., Billen, L. P., Bindner, S., Shamas-Din, A., Fradin, C., Leber, B., and Andrews, D. W. (2008) *Cell* **135,** 1074–1084
41. Print, C. G., Loveland, K. L., Gibson, L., Meehan, T., Stylianou, A., Wreford, N., de Kretser, D., Metcalf, D., Köntgen, F., Adams, J. M., and Cory, S. (1998) *Proc. Natl. Acad. Sci. U.S.A.* **95,** 12424–12431
42. Ross, A. J., Waymire, K. G., Moss, J. E., Parlow, A. F., Skinner, M. K., Russell, L. D., and MacGregor, G. R. (1998) *Nat. Genet.* **18,** 251–256
43. Veis, D. J., Sorenson, C. M., Shutter, J. R., and Korsmeyer, S. J. (1993) *Cell* **75,** 229–240
44. Hamasaki, A., Sendo, F., Nakayama, K., Ishida, N., Negishi, I., Nakayama, K., and Hatakeyama, S. (1998) *J. Exp. Med.* **188,** 1985–1992
45. Dzhagalov, I., Dunkle, A., and He, Y. W. (2008) *J. Immunol.* **181,** 521–528
46. Jabbour, A. M., Heraud, J. E., Daunt, C. P., Kaufmann, T., Sandow, J., O'Reilly, L. A., Callus, B. A., Lopez, A., Strasser, A., Vaux, D. L., and Ekert, P. G. (2009) *Cell Death Differ.* **16,** 555–563

Biochemical and Biophysical Research Communications 412 (2011) 92–97

Contents lists available at ScienceDirect

Biochemical and Biophysical Research Communications

journal homepage: www.elsevier.com/locate/ybbrc

Alterations in microRNA expression profile in HCV-infected hepatoma cells: Involvement of miR-491 in regulation of HCV replication via the PI3 kinase/Akt pathway

Hisashi Ishida [a], Tomohide Tatsumi [a], Atsushi Hosui [a], Takatoshi Nawa [a], Takahiro Kodama [a], Satoshi Shimizu [a], Hayato Hikita [a], Naoki Hiramatsu [a], Tatsuya Kanto [a], Norio Hayashi [b], Tetsuo Takehara [a,*]

[a] Department of Gastroenterology and Hepatology, Osaka University Graduate School of Medicine, 2-2, Yamadaoka, Suita 565-0871, Japan
[b] Kansai Rosai Hospital, 3-1-69, Inabaso, Amagasaki 660-8511, Japan

ARTICLE INFO

Article history:
Received 5 July 2011
Available online 23 July 2011

Keywords:
MicroRNA
Hepatitis C virus
PI3 kinase/Akt pathway

ABSTRACT

The aim of this study was to investigate the role of microRNA (miRNA) on hepatitis C virus (HCV) replication in hepatoma cells. Using miRNA array analysis, miR-192/miR-215, miR-194, miR-320, and miR-491 were identified as miRNAs whose expression levels were altered by HCV infection. Among them, miR-192/miR-215 and miR-491 were capable of enhancing replication of the HCV replicon as well as HCV itself. HCV IRES activity or cell proliferation was not increased by forced expression of miR-192/miR-215 or miR-491. Investigation of signaling pathways revealed that miR-491 specifically suppressed the phosphoinositol-3 (PI3) kinase/Akt pathway. Under inhibition of PI3 kinase by LY294002, the suppressive effect of miR-491 on HCV replication was abolished, indicating that suppression of HCV replication by miR-491 was dependent on the PI3 kinase/Akt pathway. miRNAs altered by HCV infection would then affect HCV replication, which implies a complicated mechanism for regulating HCV replication. HCV-induced miRNA may be involved in changes in cellular properties including hepatocarcinogenesis.

1. Introduction

Hepatitis C virus (HCV) is a major causative agent of liver diseases worldwide. Elimination of HCV fails in about 80% of infected patients, which leads to chronic hepatitis, liver cirrhosis, and subsequent development of hepatocellular carcinoma [1]. Combination therapy of pegylated-interferon-α and ribavirin results in sustained clearance of serum HCV-RNA in only ~50% of patients [2,3]. To improve therapeutic efficacy of the virologic response rate, drugs inhibiting the functions of HCV proteins such as NS3, NS5A, and NS5B, are currently under development. Although a number of studies have clarified the mechanisms of the effect of HCV on infected cells or the role of host factors on regulation of HCV replication, there remains much to be investigated.

MicroRNAs (miRNAs) were identified as a population of small RNAs, modulating translation by binding to sites of antisense complementarity in 3′ untranslated regions of target mRNA [4]. With respect to regulation of HCV replication, the relevance of several miRNAs has been recently reported. miR-122, a hepatocyte-specific miRNA, was identified as a positive regulatory factor for HCV replication by binding to two sites in the HCV genome [5]. Each of the interferon-β-induced miRNAs, miR-196, miR-296, miR-351, miR-431, and miR-448, has a partially complementary sequence to HCV, resulting in suppression of HCV replication [6]. Thus, a miRNA with homology to the HCV sequence is likely to have the ability to regulate HCV. Another possible mechanism of miRNA regulation of HCV replication is the targeting of some cellular gene involved in HCV replication. miR-141 was shown to suppress DLC-1 leading to efficient HCV replication [7]. Although some miRNAs were shown to be capable of regulating HCV replication, details of the relationship between miRNAs and HCV replication are still largely unknown.

In the present study, we performed miRNA array analysis to identify miRNA(s) altered by HCV infection in Huh7, a hepatoma cell line. We further investigated whether HCV-regulated miRNA could, in turn, affect HCV replication. As a result, we were able to identify five miRNAs: miR-192 and its homolog miR-215 and miR-194 as upregulated miRNAs and miR-320 and miR-491 as downregulated miRNAs. Among them, miR192/miR-215 and miR-491 enhanced HCV replication in HCV replicon cells as well as in cell culture-infectious HCV (HCVcc)-infected cells. miR-192/miR215 and miR-491 did not increase cell proliferation or HCV internal ribosome entry site (IRES) activity, suggesting that these were not the reasons for increased HCV replication. Further investigation revealed that miR-491 suppressed the PI3 kinase/Akt

* Corresponding author. Fax: +81 6 6879 3629.
E-mail address: takehara@gh.med.osaka-u.ac.jp (T. Takehara).

0006-291X/$ - see front matter © 2011 Elsevier Inc. All rights reserved.
doi:10.1016/j.bbrc.2011.07.049

pathway suggesting that this could be responsible for augmentation of HCV replication by miR-491.

2. Materials and methods

2.1. Cells, antibodies

The hepatoma-derived cell line Huh7 was maintained in DMEM supplemented with 10% FCS. The HCV subgenomic cell line Huh-RepSI, harboring HCV-N (genotype 1b), was previously described [8]. Antibodies to phospho-ERK (Thr202/Tyr204), Akt, phospho-Akt (Ser473) were purchased from Cell Signaling Technology. An antibody to β-actin (A-5441) was from Sigma–Aldrich. A mouse monoclonal antibody to HCV core protein (C7-50) was obtained from Affinity BioReagents. A mouse monoclonal antibody to HCV NS5A (clone 388) was from Meridian Life Science, Inc. LY294002, a PI3 kinase inhibitor, was obtained from Calbiochem.

2.2. Immunoblot analysis

Total cellular protein was extracted with lysis buffer containing 1% Nonidet P-40, 0.5% sodium deoxycholate, 0.1% SDS, 1 mM sodium vanadate, 50 mM NaF, and protease inhibitor cocktail (Nacalai Tesque, Japan) in phosphate-buffered saline. Protein samples were separated by SDS–polyacrylamide gel electrophoresis and transferred to a polyvinylidene difluoride membrane (Bio-Rad). After blocking, the membrane was probed with specific primary antibodies, followed by further incubation with a secondary antibody conjugated with horseradish peroxidase (GE Healthcare). Proteins were visualized using ECL Western blot detection reagents (GE Healthcare) and exposure to film.

2.3. miRNA transfection

Synthesized miRNAs, miR-192, miR-194, miR-215, miR-320, miR-491, and negative control miRNA were purchased from Thermo Fisher Scientific. Cells (2×10^5 per well) were seeded into 6-well plates, transfected with miRNA at a concentration of 10 nM using Lipofectamine RNAiMAX (Invitrogen) according to manufacturer's instruction. After incubation for 2 days, the cells were harvested and assayed by immunoblot or real-time RT-PCR analysis.

2.4. Dual luciferase assay

We used a dicistronic plasmid, pRLHL, to investigate the effects of miRNAs on HCV IRES (Fig. 2A) [9]. Huh7 cells (1×10^6 cells in a 10-cm dish) were transfected with 10 μg of pRLHL using FuGene6 (Roche). After 24 h, the cells were seeded into 24-well plates (5×10^4 cells per well) and transfected with miRNA or negative control at a concentration of 10 nM as described above. After incubation for 2 days, cells were lysed, and assayed for HCV IRES-dependent firefly luciferase activity and cap-dependent renilla luciferase activity using the Dual Luciferase Reporter Assay System (Promega).

2.5. Cell culture-infectious HCV

HJ3-5(YH/QL) is a chimeric cell culture-infectious virus with a genome consisting of the core to NS2 sequence of genotype 1a (H77) virus placed within the background of the genotype 2a JFH1 virus, and containing compensatory mutations in E1 (Y361H) and NS3 (Q1251L) [10]. Virus stock (10^7 focus-forming units (FFU)/ml) was prepared as described previously [11].

For HCV infection, Huh7 cells (2×10^5 per well) were seeded into 6-well plates. After overnight incubation, the medium was replaced with 1 ml medium containing 4×10^5 FFU virus (the infection was carried out at an m.o.i. of ~2). After 12 h incubation, the cells were washed with PBS and re-fed with normal culture medium. At 5 days after inoculation with the virus, total RNA was obtained from the cells using Trizol (Invitrogen).

2.6. Real-time reverse transcription-polymerase chain reaction (RT-PCR)

Total RNA was extracted from the cells with RNAeasy (QIAGEN). The RNA, 1 μg, was reverse transcribed with High Capacity RNA-to-cDNA Master Mix (Applied Biosystems) in a 20 μl reaction, then 1 μl of the reaction was subjected to real-time PCR assay using TaqMan Gene Expression Assays (Applied Biosystems).

2.7. Cell proliferation assay

Cell proliferation was assessed by WST-1 (2-[2-methoxy-4-nitrophenyl]-3-[4-nitrophenyl]-5-[2,4-disulpho-phenyl]-2H-tetrazolium, monosodium salt) assay according to the manufacturer's suggested protocol (Nacalai Tesque). Briefly, Huh7 cells (1×10^4 per well) were seeded into 96-well flat-bottom plates, transfected with synthesized miRNA or negative control as above, and cultured in DMEM containing 10% FBS. WST-1 reagent, 10 μl, was added to each well, the cells were incubated at 37 °C for 1 h, and absorbance at 450 nm was measured using a spectrophotometer.

2.8. miRNA array analysis

To screen for miRNA affected by HCV infection, we performed microarray analysis using *mir*Vana miRNA Bioarray V9.2 (Ambion), which carries genes for a total 633 kinds of miRNAs containing 471 human genes, 380 mouse genes and 238 rat genes. Using the flash PAGE system (Ambion), miRNA was purified from 22 μg total RNA extracted from HCVcc-infected cells or mock-infected cells. The purified miRNA samples from HCVcc-infected cells and mock-infected cells were labeled with Cy3 and Cy5, respectively, using mirVana miRNA Labeling kit (Ambion) and CyeDye Mono-Reactive Dye Pack (GE Healthcare Biosciences). The labeled miRNA was hybridized to the array for ~16 h at 42 °C. After hybridization, the array was washed with Low Stringency Wash (Ambion) once and High Stringency Wash (Ambion) twice. Next, the array was dried with centrifugation at 600*g* for 3 min and scanned with GenePix 4000B scanner (Axon Instruments, CA, USA). The signal data were calculated with an Array-Pro Analyzer ver. 4.5 (Media Cybernetics, Inc.). The array data were normalized by global normalization using the Microarray Data Analysis Tool (Filgen, Inc.).

3. Results

3.1. Identification of miRNAs regulated by HCV infection

Huh7 cells were infected with HCVcc at ~2 m.o.i. After incubation for 5 days, total RNA was extracted from the cells followed by purification with small RNA and miRNA array analysis. A portion of the cells was subjected to immunofluorescence analysis for staining of HCV core protein to verify that more than 90% of the cells were infected with HCV. The ratio of Cy3 intensity to Cy5 intensity was calculated and alteration of the miRNA expression profile was analyzed. A ratio of more than 1.5-fold increase/decrease was considered to be altered. To exclude miRNAs with low expression levels, those with a net intensity of Cy3 and Cy5 of more than 1000 were picked out. As a result, the miRNAs of miR-192, miR-194, miR-320, and miR-491 were identified as altered miRNAs (Table 1). miR-192 and miR-194 were up-regulated by HCV infection,

Table 1
miRNAs altered by HCV infection.

miRNA	Intensity				Sequence
	Cy3 (HCV)	Cy5 (mock)	Net	Cy3/Cy5	
miR-192	987.90	607.05	1594.95	1.63	CUGACCUAUGAAUUGACAGCC
miR-194	793.48	498.00	1291.48	1.59	UGUAACAGCAACUCCAUGUGGA
miR-215	156.21	69.39	225.60	2.25	AUGACCUAUGAAUUGACAGAC
miR-320	897.44	1401.93	2299.37	0.64	AAAAGCUGGGUUGAGAGGGCGAA
miR-491	925.38	2495.47	3420.85	0.37	AGUGGGGAACCCUUCCAUGAGGA

and miR-320 and miR-491 were down-regulated. In addition, miR-215, whose net expression while relatively low, was also studied in the subsequent investigation as an upregulated miRNA because it is considered to be a cousin of miR-192 (see their homologous sequences in Table 1). miR-215 showed a high induction level, and miR-192 and miR-215 were reported to have common induction mechanisms and target genes [12,13].

3.2. Regulation of HCV replication by miRNAs

Next, we checked whether the miRNAs were capable of regulating HCV replication. To assess this, we transfected Huh-RepSI, a HCV subgenomic replicon cell line, with synthesized miRNAs, and then monitored HCV RNA abundance and NS5A protein abundance using real-time RT-PCR and immunoblot analysis, respectively. Among the five miRNAs tested, miR-192/miR-215 and miR-491 significantly increased replicon abundance (Fig. 1A and B), while miR-194 and miR-320 did not show any significant change. HCV subgenomic replicon RNA contains the NS3 through NS5B region, which is required for genome RNA replication, but not for virus particle production. To confirm that the effect of the miRNAs was reproducible in a system equipped with the entire HCV life cycle, we used Huh7 cells infected with HCVcc. As expected, HCV abundance was upregulated by the three miRNAs in the HCVcc-infected cells similarly to HCV replicon cells (Fig. 1C and D). In addition, the HCV strain used in the experiment was a chimera of genotype 1a (H77, core to NS2) and genotype 2 (JFH-1, NS3 to NS5B) [10]. In particular, the genotype of the replication machinery of the virus (namely, NS3 to NS5B) was JFH-1. This differed from that of Huh-RepSI (HCV-N, genotype 1b) [8], which suggests that the enhancing effect of miR-192/miR-215 and miR-491 on HCV genome replication was not genotype-specific.

3.3. Effect of miRNAs on HCV IRES, cell proliferation

Since miR-192/miR-215 and miR-491 were shown to be capable of enhancing HCV replication, we next tried to elucidate how they regulate it. First, we examined whether the miRNAs can regulate HCV IRES activity. In this experiment, we transfected replicon cells with a dicistronic vector, pRLHL [9], which contained the firefly luciferase gene driven by HCV IRES and the renilla luciferase gene translated in a cap-dependent manner which was used as a control of general translational activity (Fig. 2A). After 24 h, the miRNAs were transfected, then luciferase activities induced by HCV IRES and cap translation were measured at 2 days after

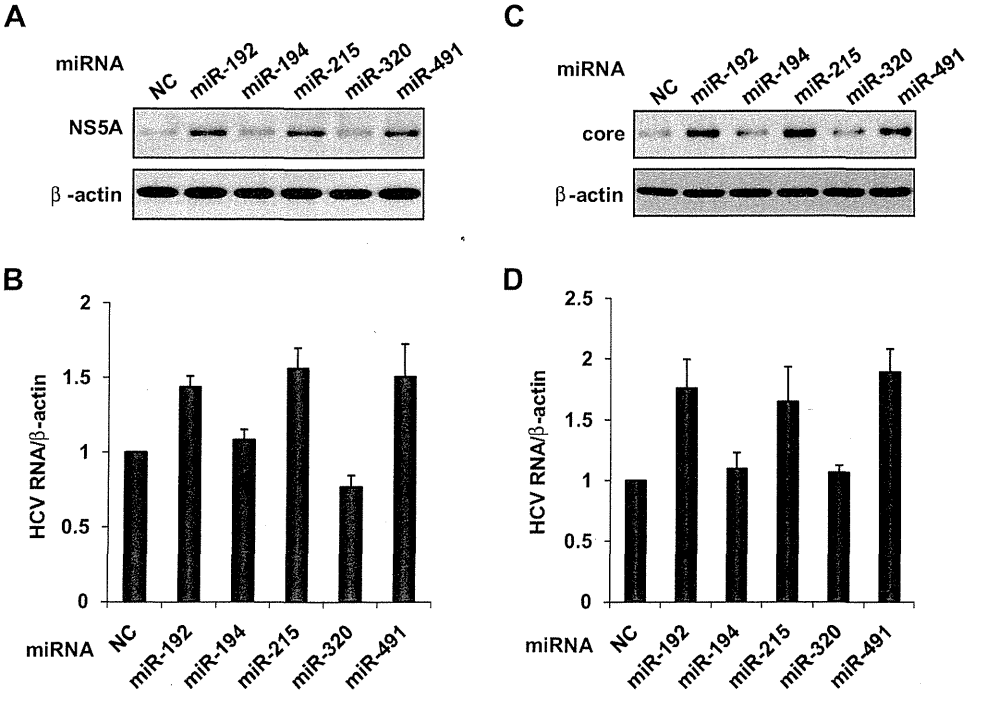

Fig. 1. Regulation of HCV replicon or HCVcc abundance by miRNAs. Cells of Huh-RepSI, a HCV subgenomic replicon, were transfected with synthesized miRNAs and assayed for NS5A protein expression (A) or HCV RNA abundance (B). HCVcc-infected Huh7 cells were transfected with synthesized miRNAs and assayed for core protein expression (C) or HCV RNA abundance (D). NC: negative control miRNA.

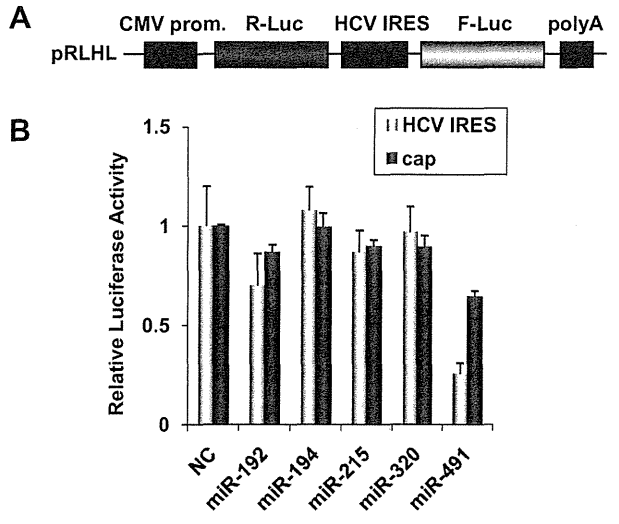

Fig. 2. Regulation of HCV IRES and cap-dependent translation by miRNAs. Huh-RepSI cells were transfected with a dicistronic vector, pRLHL (A), incubated for 24 h. The cells were seeded to 24-well plates and transfected with the miRNAs. After further incubation for 2 days, the cells were harvested and assayed for dual luciferase activity (B).

transfection (Fig. 2B). In this assay, activation of IRES was determined by the ratio of IRES-dependent luciferase activity to cap-dependent luciferase activity. Interestingly, none of the miRNAs could increase the HCV IRES activity. miR-491 suppressed cap-dependent translation and showed more suppression of HCV IRES activity. Thus, these results indicated that there was some mechanism upregulating HCV replication other than regulation of IRES activity.

Previous work demonstrated that HCV replication was affected by cell proliferation [14]. This led us to access the effects of the miRNAs on cell proliferation. Compared to negative control miRNA-transfected cells, however, none of the transfectants of the miRNAs, including those which increased HCV replication, revealed upregulation of cell proliferation, and miR-491 even suppressed it (Fig. 3). Therefore, regulation of cell proliferation was not the reason for the increase of HCV replication. The effect of miR-491 of suppressing cell growth was likely to be caused by inhibition of general translation as shown in Fig. 2B.

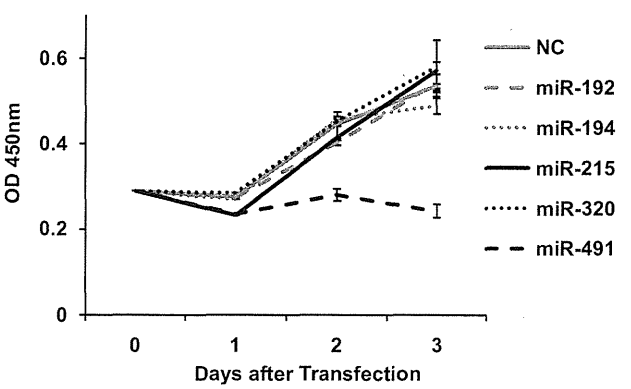

Fig. 3. Regulation of cell proliferation by miRNAs. Huh7 cells were seeded into 96-well plates, transfected with the miRNAs. At day 0, 1, 2, and 3 after transfection, the cells were subjected to WST-1 assay as described in Section 2.

3.4. Effect of miRNAs on intracellular signaling

To clarify the mechanism of the regulation of HCV replication, we next focused our investigation on intracellular signaling pathways. Previous studies have reported that HCV replication is regulated by intracellular signaling pathways, such as ERK [15], p38 [8], PI3 kinase/Akt [11], and smad [16], in addition to JAK/STAT. Since transfection of the miRNAs had no effect on the JAK/STAT signaling pathway (data not shown), we examined the phosphorylation of ERK and Akt. Because both showed a suppressing effect on HCV replication, suppression of the pathway was anticipated in cells in which HCV replication was enhanced. As shown in Fig. 4A, phosphorylation of Akt at Ser-473 was markedly suppressed in the cells transfected with miR-491, while no significant inhibition of ERK activity was observed. To further investigate the relevance of the PI3 kinase/Akt pathway to miR-491-induced upregulation of HCV replication, we used LY294002, a PI3 kinase inhibitor. When the PI3 kinase pathway was blocked by this reagent, the HCV RNA level was enhanced up to 2-fold. miR-491 transfection also resulted in an increase of HCV abundance, though the effect was less

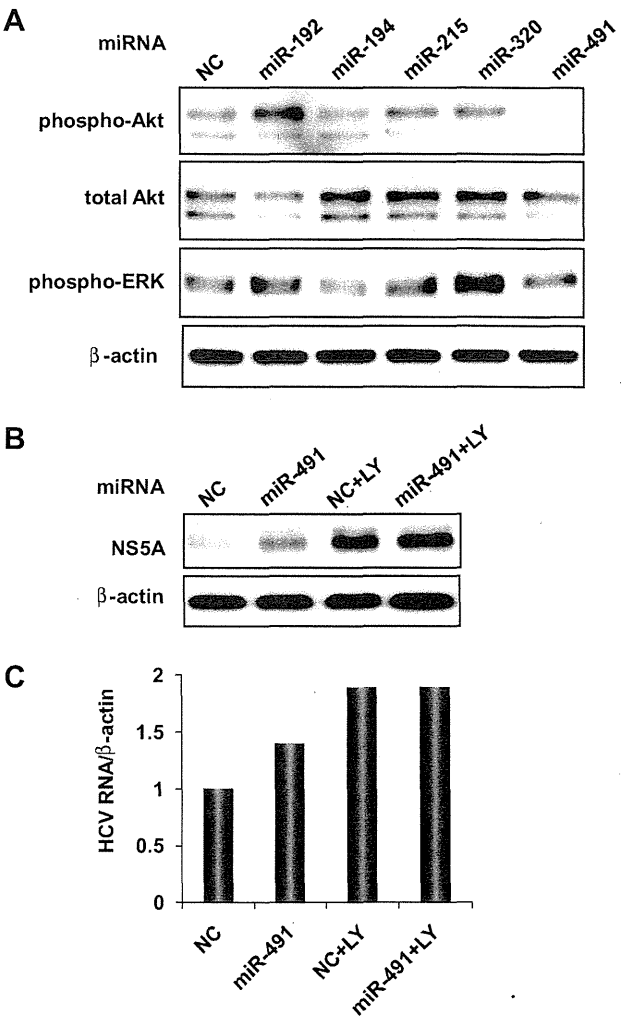

Fig. 4. Involvement of Akt suppression in miR-491-mediated upregulation of HCV replication. (A) Immunoblot analysis of miRNA-transfected HCV replicon cells using antibodies to Akt, phospho-Akt, phospho-ERK and β-actin. (B and C) HCV replicon cells were transfected with miR-491 or treated with Akt inhibitor, and assayed for NS5A protein abundance (B) or HCV RNA abundance (C). LY: LY294002.

than that of LY294002, presumably because of incomplete inhibition of Akt. When miR-491 transfected cells were cultured in the presence of LY294002, the HCV replication level was enhanced to the same extent as that in the LY294002-treated cells with negative control miRNA. Since no additive effect of miR-491 was observed under strong blockade of the PI3 kinase/Akt pathway, inhibition of this pathway was likely to be responsible for the miR-491-induced upregulation of HCV replication.

4. Discussion

In the present study, we tried to identify the miRNA(s) affected by HCV infection and establish how they influence HCV replication. Five miRNAs, miR-192, miR-194, miR-215, miR-320, and miR-491, were identified as HCV-regulated miRNAs by miRNA array analysis. Three upregulated miRNAs, miR-192, miR-194, and miR-215, were previously identified as p53-inducible miRNAs [12,13]. Two miRNA clusters which encode identical miR-194 sequences (i.e., the miR-194-2/miR-192 cluster on chromosome 11 and the miR-194-1/miR-215 cluster on chromosome 1) contain two closely related miRNAs, miR-192 and miR-215, suggesting that their expressions are regulated similarly which led to their simultaneous identification. miR-192/miR-194/miR-215 are known to act as tumor-suppressing miRNAs by inducing cell cycle arrest [12]. In Huh7 cells, however, the p53 function is believed to be abolished by a point mutation at codon 220. Therefore, the upregulation of miR-192/miR-194/miR-215 was likely to be exerted in a p53-independent manner. Since miR-192 and miR-194 are considered to be substantially expressed in human liver tissue [17] and there are several reports about the suppression of p53 function by HCV (reviewed in Ref. [18]), the result may not necessarily be the same if the investigation is conducted in human hepatocytes or in cells with intact p53 activity.

The downregulated miRNAs, miR-320 and miR-491, are considered to be relevant to carcinogenesis. miR-320 induces G1 arrest and suppresses cell proliferation by targeting CDK6 [19], CD71 [20], IGF1 [21] and induces apoptosis by suppressing Bcl-2 and Mcl-1 [22]. miR-491 is also capable of inducing apoptosis by targeting Bcl-xL [23], which is often upregulated in HCC tissues [24]. In this study, we showed that miR-491 inhibited the PI3 kinase/Akt pathway, which is one of the important pathways leading to cancerous properties. Importantly, miR-320 was identified as one of the significantly repressed miRNAs in CH-B, CH-C, and HCC compared with normal liver tissue [25]. Although the details of the relevance of miR320 and miR-491 to hepatocarcinogenesis have not yet been clarified, as these two miRNAs have a tendency to suppress genes related to carcinogenesis, their downregulation in HCV-infected cells may play some role in hepatocarcinogenesis.

Thus far, several miRNAs have been reported to regulate HCV replication. miR-122 was shown to be a direct activating factor for HCV replication [5], but alteration of this miRNA was not observed in response to HCV infection in this study. IFN-β-induced miRNAs, miR-196, miR-296, miR-351, miR-431 and miR-448, have been identified as anti-HCV miRNAs [6]. These miRNAs are able to regulate HCV replication by direct interaction with HCV genome RNA. In the case of miR-192/miR-215, there are several sites in the HCV genome sequence which show weak homology to the miRNAs (data not shown). Although the possibility of miR-192/miR-215 binding to the HCV genome and regulating replication cannot completely be excluded, this seems unlikely because the homologous sequence to miR-192/miR-215 cannot be found in the UTR region like miR-122 and direct binding to RNA usually suppresses the RNA function for protein synthesis. There is, however, a very rare case of miR-122-mediated facilitation of HCV replication by binding to two sites within the HCV genome.

Although the mechanism of miR-491-mediated suppression of the PI3 kinase pathway is not clear, it was speculated that some gene involved in Akt activation was the target of miR-491. However, the candidate of the target gene was not clearly found in the list of putative target genes of miR-491 revealed by in silico analysis. We tried to evaluate the mRNA levels of upstream genes of Akt, such as the genes which belong to the family of PI3 kinase, PTEN, growth factor receptors, using the RT-PCR method, but none of them was affected by miR-491 (data not shown). Nevertheless, investigation of target genes of miR-491 should be of interest for the field of oncology because here we have shown that miR-491 suppresses Akt, which is a factor closely related to various types of cancer via cell survival. Also, it has been demonstrated that miR-491 can induce apoptosis by ablating Bcl-xL [23]. Indeed, our observation that cell viability was significantly suppressed by forced expression of miR-491 presumably via decrease of Akt signaling suggests the anti-oncogenic feature of miR-491. Further study of the mechanism of miR-491, its target genes, and expression pattern in cancer tissue remain to be performed.

In conclusion, we showed altered expression profiles of miRNAs by HCV infection, and some of them were capable of regulating HCV replication, which may represent a complicated mechanism of HCV replication. A number of studies have demonstrated regulation of many cellular factors by miRNAs, which results in modulation of cellular functions including cell growth, apoptosis, cellular stresses, metabolism, and carcinogenesis. The miRNAs identified in this study may also be involved in changes in the phenotype of HCV-infected cells.

Acknowledgment

We thank Stanley Lemon for providing the plasmid pRLHL and the cell culture-infectious virus HJ3-5(YH/QL).

References

[1] L.B. Seeff, Natural history of hepatitis C, Hepatology 26 (1997) 21S–28S.
[2] M.W. Fried, M.L. Shiffman, K.R. Reddy, C. Smith, G. Marinos, F.L. Goncales Jr., D. Haussinger, M. Diago, G. Carosi, D. Dhumeaux, A. Craxi, A. Lin, J. Hoffman, J. Yu, Peginterferon alfa-2a plus ribavirin for chronic hepatitis C virus infection, N. Engl. J. Med. 347 (2002) 975–982.
[3] S.J. Hadziyannis, H. Sette Jr., T.R. Morgan, V. Balan, M. Diago, P. Marcellin, G. Ramadori, H. Bodenheimer Jr., D. Bernstein, M. Rizzetto, S. Zeuzem, P.J. Pockros, A. Lin, A.M. Ackrill, Peginterferon-alpha2a and ribavirin combination therapy in chronic hepatitis C: a randomized study of treatment duration and ribavirin dose, Ann. Intern. Med. 140 (2004) 346–355.
[4] M. Lagos-Quintana, R. Rauhut, W. Lendeckel, T. Tuschl, Identification of novel genes coding for small expressed RNAs, Science 294 (2001) 853–858.
[5] C.L. Jopling, M. Yi, A.M. Lancaster, S.M. Lemon, P. Sarnow, Modulation of hepatitis C virus RNA abundance by a liver-specific microRNA, Science 309 (2005) 1577–1581.
[6] I.M. Pedersen, G. Cheng, S. Wieland, S. Volinia, C.M. Croce, F.V. Chisari, M. David, Interferon modulation of cellular microRNAs as an antiviral mechanism, Nature 449 (2007) 919–922.
[7] K. Banaudha, M. Kaliszewski, T. Korolnek, L. Florea, M.L. Yeung, K.T. Jeang, A. Kumar, MicroRNA silencing of tumor suppressor DLC-1 promotes efficient hepatitis C virus replication in primary human hepatocytes, Hepatology 53 (2011) 53–61.
[8] H. Ishida, K. Ohkawa, A. Hosui, N. Hiramatsu, T. Kanto, K. Ueda, T. Takehara, N. Hayashi, Involvement of p38 signaling pathway in interferon-alpha-mediated antiviral activity toward hepatitis C virus, Biochem. Biophys. Res. Commun. 321 (2004) 722–727.
[9] T.H. Wang, R.C. Rijnbrand, S.M. Lemon, Core protein-coding sequence but not core protein modulates the efficiency of cap-independent translation directed by the internal ribosome entry site of hepatitis C virus, J. Virol. 74 (2000) 11347–11358.
[10] M. Yi, Y. Ma, J. Yates, S.M. Lemon, Compensatory mutations in E1 p7 NS2 and NS3 enhance yields of cell culture-infectious intergenotypic chimeric hepatitis C virus, J. Virol. 81 (2007) 629–638.
[11] H. Ishida, K. Li, M. Yi, S.M. Lemon, p21-activated kinase 1 is activated through the mammalian target of rapamycin/p70 S6 kinase pathway and regulates the replication of hepatitis C virus in human hepatoma cells, J. Biol. Chem. 282 (2007) 11836–11848.

[12] C.J. Braun, X. Zhang, I. Savelyeva, S. Wolff, U.M. Moll, T. Schepeler, T.F. Orntoft, C.L. Andersen, M. Dobbelstein, p53-Responsive micrornas 192 and 215 are capable of inducing cell cycle arrest, Cancer Res. 68 (2008) 10094–10104.
[13] S.A. Georges, M.C. Biery, S.Y. Kim, J.M. Schelter, J. Guo, A.N. Chang, A.L. Jackson, M.O. Carleton, P.S. Linsley, M.A. Cleary, B.N. Chau, Coordinated regulation of cell cycle transcripts by p53-Inducible microRNAs miR-192 and miR-215, Cancer Res. 68 (2008) 10105–10112.
[14] M. Honda, S. Kaneko, E. Matsushita, K. Kobayashi, G.A. Abell, S.M. Lemon, Cell cycle regulation of hepatitis C virus internal ribosomal entry site-directed translation, Gastroenterology 118 (2000) 152–162.
[15] T. Murata, M. Hijikata, K. Shimotohno, Enhancement of internal ribosome entry site-mediated translation and replication of hepatitis C virus by PD98059, Virology 340 (2005) 105–115.
[16] T. Murata, T. Ohshima, M. Yamaji, M. Hosaka, Y. Miyanari, M. Hijikata, K. Shimotohno, Suppression of hepatitis C virus replicon by TGF-beta, Virology 331 (2005) 407–417.
[17] O. Barad, E. Meiri, A. Avniel, R. Aharonov, A. Barzilai, I. Bentwich, U. Einav, S. Gilad, P. Hurban, Y. Karov, E.K. Lobenhofer, E. Sharon, Y.M. Shiboleth, M. Shtutman, Z. Bentwich, P. Einat, MicroRNA expression detected by oligonucleotide microarrays: system establishment and expression profiling in human tissues, Genome Res. 14 (2004) 2486–2494.
[18] M. Anzola, J.J. Burgos, Hepatocellular carcinoma: molecular interactions between hepatitis C virus and p53 in hepatocarcinogenesis, Expert Rev. Mol. Med. 5 (2003) 1–16.
[19] H. Duan, Y. Jiang, H. Zhang, Y. Wu, MiR-320 and miR-494 affect cell cycles of primary murine bronchial epithelial cells exposed to benzo[a]pyrene, Toxicol. In Vitro 24 (2010) 928–935.
[20] D.G. Schaar, D.J. Medina, D.F. Moore, R.K. Strair, Y. Ting, miR-320 targets transferrin receptor 1 (CD71) and inhibits cell proliferation, Exp. Hematol. 37 (2009) 245–255.
[21] X.H. Wang, R.Z. Qian, W. Zhang, S.F. Chen, H.M. Jin, R.M. Hu, MicroRNA-320 expression in myocardial microvascular endothelial cells and its relationship with insulin-like growth factor-1 in type 2 diabetic rats, Clin. Exp. Pharmacol. Physiol. 36 (2009) 181–188.
[22] L. Chen, H.X. Yan, W. Yang, L. Hu, L.X. Yu, Q. Liu, L. Li, D.D. Huang, J. Ding, F. Shen, W.P. Zhou, M.C. Wu, H.Y. Wang, The role of microRNA expression pattern in human intrahepatic cholangiocarcinoma, J. Hepatol. 50 (2009) 358–369.
[23] H. Nakano, T. Miyazawa, K. Kinoshita, Y. Yamada, T. Yoshida, Functional screening identifies a microRNA, miR-491 that induces apoptosis by targeting Bcl-X(L) in colorectal cancer cells, Int. J. Cancer 127 (2010) 1072–1080.
[24] T. Takehara, X. Liu, J. Fujimoto, S.L. Friedman, H. Takahashi, Expression and role of Bcl-xL in human hepatocellular carcinomas, Hepatology 34 (2001) 55–61.
[25] S. Ura, M. Honda, T. Yamashita, T. Ueda, H. Takatori, R. Nishino, H. Sunakozaka, Y. Sakai, K. Horimoto, S. Kaneko, Differential microRNA expression between hepatitis B and hepatitis C leading disease progression to hepatocellular carcinoma, Hepatology 49 (2009) 1098–1112.

Biochemical and Biophysical Research Communications 406 (2011) 614–620

Contents lists available at ScienceDirect

Biochemical and Biophysical Research Communications

journal homepage: www.elsevier.com/locate/ybbrc

Involvement of STAT3-regulated hepatic soluble factors in attenuation of stellate cell activity and liver fibrogenesis in mice

Minoru Shigekawa [a], Tetsuo Takehara [a,*], Takahiro Kodama [a], Hayato Hikita [a], Satoshi Shimizu [a], Wei Li [a], Takuya Miyagi [a], Atsushi Hosui [a], Tomohide Tatsumi [a], Hisashi Ishida [a], Tatsuya Kanto [a], Naoki Hiramatsu [a], Norio Hayashi [b]

[a] Department of Gastroenterology and Hepatology, Osaka University Graduate School of Medicine, Suita, Osaka, Japan
[b] Kansai Rosai Hospital, Amagasaki, Hyogo, Japan

ARTICLE INFO

Article history:
Received 19 February 2011
Available online 26 February 2011

Keywords:
STAT3
Liver fibrosis
Hepatic stellate cells
Acute phase proteins

ABSTRACT

Glycoprotein 130 (gp130)/signal transducer and activator of transcription 3 (STAT3) signaling in hepatocytes controls a variety of physiological and pathological processes including liver regeneration, apoptosis resistance and metabolism. Recent research has shed light on the importance of acute phase proteins (APPs) regulated by hepatic gp130/STAT3 in host defense through suppression of innate immune responses during systemic inflammation. To examine whether these STAT3-regulated soluble factors directly affect liver fibrogenic responses during liver injury, hepatocyte-specific STAT3 knockout (L-STAT3 KO) mice and control littermates were subjected to bile duct ligation (BDL) and examined 10 days later. In contrast to controls, L-STAT3 KO mice failed to produce APPs, such as serum amyloid A and haptoglobin, after BDL. Whereas L-STAT3 KO mice displayed similar levels of cholestasis, inflammatory cell infiltration and regeneration in the liver, they developed exacerbated liver injury and fibrosis with significant increases in expression of alpha-smooth muscle actin and type I collagen genes. *In vitro* experiments revealed that attenuated expression of APPs in primary hepatocytes isolated from L-STAT3 KO mice with IL-6 exposure, compared to wild-type hepatocytes. The cultured supernatant from IL-6-treated wild-type hepatocytes inhibited expression of alpha-smooth muscle actin and type I collagen genes in activated hepatic stellate cells (HSCs), whereas this did not occur with the supernatant from IL-6-treated knockout hepatocytes or with control medium. In conclusion, the absence of STAT3 in hepatocytes leads to exacerbation of liver fibrosis during cholestasis. Soluble factors released from hepatocytes, dependent on STAT3, collectively play a protective role in liver fibrogenesis through an inhibitory effect on activated HSCs.

1. Introduction

Cholestatic liver injury is characterized by bile flow impairment of different parts of the biliary tree, which can be caused by gallstones, autoimmunity or unknown etiology. Persistent cholestasis eventually progresses toward biliary fibrosis and cirrhosis because of bile acid-induced cholangiocyte and hepatocyte damage, leading to failure of cellular repopulation and excessive deposition of extracellular matrix (ECM) proteins. Hepatic stellate cells (HSCs) are the main ECM-producing cells in the injured liver [1]. Following chronic injury, HSCs activate or transdifferentiate into myofibroblast-like cells, acquiring contractile, proinflammatory and fibrogenic properties. Activated HSCs produce and deposit ECM proteins in the pericentral and periportal regions.

The signal transducer and activator of transcription 3 (STAT3) is known to be ubiquitously expressed in a wide range of tissues where it is activated by tyrosine phosphorylation in response to a variety of cytokines and growth factors (e.g. interleukin (IL)-6 family, IL-10, leptin, IL-17, IL-23, interferons and EGF). STAT3, formerly known as acute phase response factor, regulates the expression of genes involved in the acute phase response, a series of inflammatory reactions induced in response to infection and tissue

Abbreviations: ECM, extracellular matrix; HSCs, hepatic stellate cells; STAT, signal transducer and activator of transcription; IL, interleukin; gp, glycoprotein; APPs, acute phase proteins; L-STAT3 KO, hepatocyte-specific STAT3 knockout; WT, wild-type; BDL, bile duct ligation; TUNEL, terminal deoxynucleotidyl transferase-mediated deoxyuridine triphosphate nick-end labeling; BrdU, 5-bromo-2-deoxyuridine; rtPCR, reverse-transcription polymerase chain reaction; SAA, serum amyloid A; αSMA, alpha-smooth muscle actin; TGFβ, transforming growth factor beta; PDGF, platelet derived growth factor; ALT, alanine aminotransferase.

* Corresponding author. Address: Department of Gastroenterology and Hepatology, Osaka University Graduate School of Medicine, 2-2 Yamada-oka, Suita, Osaka 565-0871, Japan. Fax: +81 6 6879 3629.
E-mail address: takehara@gh.med.osaka-u.ac.jp (T. Takehara).

0006-291X/$ - see front matter © 2011 Elsevier Inc. All rights reserved.
doi:10.1016/j.bbrc.2011.02.105

injury [2]. The IL-6 family is one of the major cytokines involved in triggering the acute phase response and all members of the IL-6 family use glycoprotein 130 (gp130) as a receptor to induce nuclear translocation of STAT3 [3] as well as to activate the Ras/mitogen-activated protein (MAP) pathway. Since systemic deletion of STAT3 leads to embryonic lethality in mice, the significance of STAT3 in adult organs has been investigated using conditional knockout animals generated by the Cre/loxP recombination system [4]. Previous reports suggested that STAT3 signaling in hepatocytes controls a variety of physiological and pathological processes, including hepatocyte proliferation after partial hepatectomy [5], apoptosis resistance of hepatocytes during Fas-mediated liver injury [6] and regulation of hepatic gluconeogenic genes [7]. Further study showed that the soluble factors dependent on gp130/STAT3 signaling such as acute phase proteins (APPs) suppress innate immune cell overactivation and hypercytokinemia, leading to host-defense during systemic inflammation [8,9]. Very recently, research has shown that gp130/STAT3 signaling is protective against liver fibrogenesis by regulating inflammation and injury in the liver during chronic cholestasis [10,11]. However, it is not clear whether STAT3-dependent soluble factors from hepatocyte, such as APPs, affect the activation of HSCs and their collagen synthesis.

In the present study, we used conditional knockout mice, carrying hepatocyte-specific deletion of STAT3, and determined the effects dependent on the hepatocyte-specific STAT3 signaling pathway during cholestasis. We found that its signaling pathway offered protection from liver injury and fibrogenesis in a murine model of cholestatic liver injury. Moreover, STAT3-dependent soluble factors released from hepatocytes directly suppressed the activated HSCs and their collagen synthesis *in vitro*. Hepatocyte STAT3 signaling plays an important role in attenuation of liver disease by modulating liver damage and fibrogenesis through their collective effect on HSCs.

2. Materials and methods

2.1. Animals

Mice carrying a STAT3 gene with 2 loxP sequences flanking exon 22 have been described previously [12]. Hepatocyte-specific STAT3 knockout (L-STAT3 KO) mice were generated by crossing $STAT3^{fl/fl}$ mice with albumin-promoter Cre (Alb-Cre) transgenic mice [13]. Sex-matched $STAT3^{fl/fl}$ mice obtained from the same litter were used as wild-type (WT) controls. All mice were used at the age of 7–10 weeks. All animals were housed with 12-h light/dark cycles with free access to food and water under specific pathogen-free conditions and were treated with humane care under approval from the Animal Care and Use Committee of Osaka University Medical School.

2.2. Bile duct ligation

Bile duct ligation (BDL) is a well-established murine model of cholestasis. L-STAT3 KO mice and WT littermates were subjected to BDL as previously reported [14]. Briefly, the common bile duct was ligated 3 times with 5–0 silk sutures and then cut between the ligatures. After 10 days, the animals were sacrificed for the following analyses.

2.3. Histologic analyses

The liver sections were stained with H&E or picrosirius red. The percentage of oncotic necrosis or fibrotic area was calculated using image analysis software (win-ROOF visual system; Mitani Co., Tokyo, Japan). To assess intrahepatic macrophage accumulation, liver sections were stained with F4/80 using an anti-F4/80 rat monoclonal antibody (Abcam, Cambridge, MA). To detect apoptotic cells, the liver sections were also subjected to terminal deoxynucleotidyl transferase-mediated deoxyuridine triphosphate nick-end labeling (TUNEL) staining as previously reported [15]. To assess regenerative status, nuclear 5-bromo-2-deoxyuridine (BrdU) incorporation was evaluated as previously described [16].

2.4. Isolation and culture of murine hepatic stellate cells

HSCs were isolated from C57BL/6J mice by 2-step collagenase-pronase perfusion of mouse liver as previously described [16]. Activated HSCs after a few passages were cultured with the supernatant from primary hapatocyte or recombinant Apo-SAA (PEPROTECH, Rocky Hill, NJ).

2.5. Primary culture of hepatocytes

Hepatocytes were isolated from the liver of L-STAT3 KO mice and WT mice by 2-step collagenase-pronase perfusion of mouse liver as previously described [8]. Isolated hepatocytes were stimulated with 20 ng/ml recombinant mouse IL-6 (R&D Systems, Minneapolis, MN). The cells or the supernatant were harvested after 24 h.

2.6. Western blot analysis

Western blotting was performed as previously described [16].For immunodetection, the following antibodies were used: phospho-STAT3 (Tyr705) antibody, anti-STAT3 antibody (Cell Signaling Technology, Danvers, MA) and anti-β-actin antibody (Sigma–Aldrich, St. Louis, MO).

2.7. Real-time reverse-transcription polymerase chain reaction

Total RNA extracted from the liver tissue and HSCs were reverse transcribed and subjected to real-time reverse-transcription polymerase chain reaction (rtPCR) as previously described [15]. mRNA expression of the specific genes was quantified using TaqMan Gene Expression Assays (Applied Biosystems Inc., Foster City, CA). Assay IDs of the specific genes are provided in Supplementary Table 1. Transcript levels are presented as fold induction.

2.8. Enzyme-linked immunosorbent assay

The levels of serum amyloid A (SAA) and haptoglobin in serum and cultured supernatant were measured using SAA ELISA kit (Invitrogen, Camarillo, CA) and Mouse Haptoglobin ELISA kit (Immunology Consultants Laboratory, Newberg, OR), according to the manufacturer's protocol.

2.9. Statistical analysis

Data are presented as median and interquartile range or mean ± standard deviation, compared using the Mann–Whitney U test and unpaired *t*-test, respectively. Statistical significance was set at $p < 0.05$.

3. Results

3.1. Lack of acute phase response in L-STAT3 KO mice after BDL

L-STAT3 KO mice were produced by crossing floxed STAT3 mice and Alb-Cre transgenic mice which express Cre recombinase gene under regulation of the albumin gene promoter. To determine the

role of hepatocyte STAT3 during obstructive cholestasis, L-STAT3 KO mice and WT mice were subjected to BDL and examined 10 days later. After BDL treatment, western blot analysis revealed that STAT3 expression in the livers of L-STAT3 KO mice was greatly reduced compared with that of WT mice (Fig. 1A). In contrast to L-STAT3 KO mice, phosphorylation of STAT3 was clearly seen in WT mice with BDL compared with that in sham-operated mice (Fig. 1A). Given that STAT3 is a well-known mediator of APPs in the IL-6/gp130/STAT3 signaling pathway, we analyzed the mRNA expression of APPs such as SAA and haptoglobin by real-time rtPCR. The hepatic expression of SAA and haptoglobin genes was clearly induced after BDL in WT mice (Fig. 1B). In contrast, the hepatic expression of these genes did not increase in L-STAT3 KO mice. We also measured the serum levels of APPs. Similarly, the levels of SAA and haptoglobin clearly increased in WT littermates after BDL and were completely diminished in L-STAT3 KO mice (Fig. 1C).

3.2. L-STAT3 KO mice show progression of liver fibrosis

To examine the effect of hepatocyte-specific STAT3 deficiency on liver fibrosis after BDL, we evaluated hepatic collagen deposition by picrosirius red staining of liver sections (Fig. 2A). Morphometric analysis revealed that collagen deposition increased in both groups after BDL and was more significantly higher in L-STAT3 KO mice than in the WT littermates (Fig. 2B). As type I collagen is known to be a major form of collagen in cirrhosis, we analyzed hepatic expression of type I collagen α1 gene, *col1a1*. The levels more significantly increased in L-STAT3 KO mice than WT mice (Fig. 2C). HSCs are main collagen-producing cells in the injured liver and alpha-smooth muscle actin (αSMA) is the marker of activation of HSCs. The expression levels of αSMA gene, *acta2*, were significantly higher in L-STAT3 KO mice than WT controls after BDL (Fig. 2C). The mRNA expression of both transforming growth factor beta (TGFβ), as an important profibrogenic cytokine, and platelet derived growth factor (PDGF), which is the most potent mitogen for HSCs, were not significantly different between the two groups after BDL (Fig. 2D).

3.3. L-STAT3 KO mice display exacerbated liver injury

We examined liver injury and cholestasis upon BDL. There was no significant difference in cholestasis between the two groups after BDL as evidenced by serum levels of total bilirubin and alkaline phosphatase, but L-STAT3 KO mice showed increased levels of serum alanine aminotransferase (ALT) compared with WT controls (Fig. 3A). Oncotic necrosis, known as bile infarcts, is a characteristic feature of liver injury in the BDL model. The area of oncotic necrosis in the liver was not significantly different between the two groups after BDL (Fig. 3B). TUNEL staining of the liver sections revealed that the numbers of apoptotic cells in the liver more significantly increased in L-STAT3 KO mice than in WT littermates after BDL (Fig. 3C). We examined liver regeneration by BrdU incorporation in liver sections (Supplementary Fig. 1A). There was no significant difference between the two groups as determined by the count of BrdU-positive cells after BDL (Fig. 3D). Kupffer cells are resident macrophages that play a major role in liver inflammation by releasing cytokines. The F4/80 antigen is expressed on a wide range of mature tissue macrophages including Kupffer cells, and we thus examined F4/80 staining of liver sections (Supplementary Fig. 1B). There was no significant difference in the count of F4/80-positive cells between the two groups after BDL (Fig. 3E). The hepatic mRNA expression of CD68, expressed on monocytes/macrophages, CD4 and CD8, both of which are surface markers of T cells, was not significantly different between the two groups after BDL (Fig. 3F, Supplementary Fig. 2).

3.4. Soluble factors released from IL-6-treated hepatocytes are involved in suppression of activated HSCs and inhibition of their collagen production

In our *in vivo* study, we revealed the exacerbation of cholestasis-induced liver fibrosis and the increases in hepatic expression of αSMA and type I collagen α1 genes in L-STAT3 KO mice. Furthermore, the acute phase response induced after BDL was invisible in L-STAT3 KO mice. We hypothesized that STAT3-mediated soluble

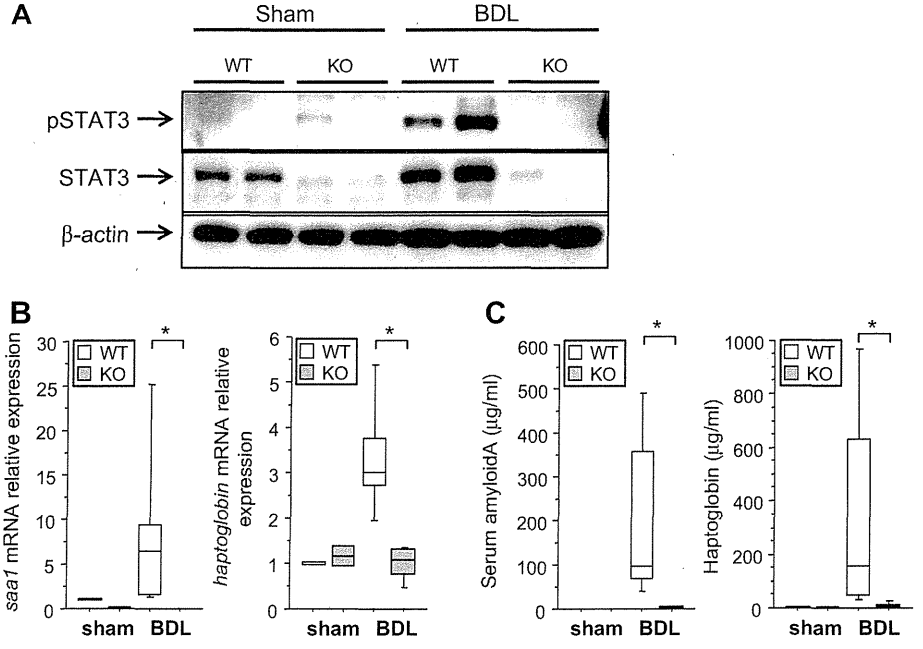

Fig. 1. Activation of STAT3 and production of acute phase proteins in the liver after BDL. L-STAT3 KO mice (KO) and WT littermates (WT) were subjected to BDL or sham-operation (sham) and examined 10 days later. (A) Expressions of STAT3 and phosphorylated STAT3 (pSTAT3) in the liver were assessed by western blot analysis. β-actin is included as a control. (B) Hepatic mRNA expression of SAA and haptoglobin was determined by real-time rtPCR analysis, $n = 8$/group, $^*p < 0.05$. (C) Serum levels of SAA and haptoglobin were determined by ELISA, $n = 8$/group, $^*p < 0.05$.

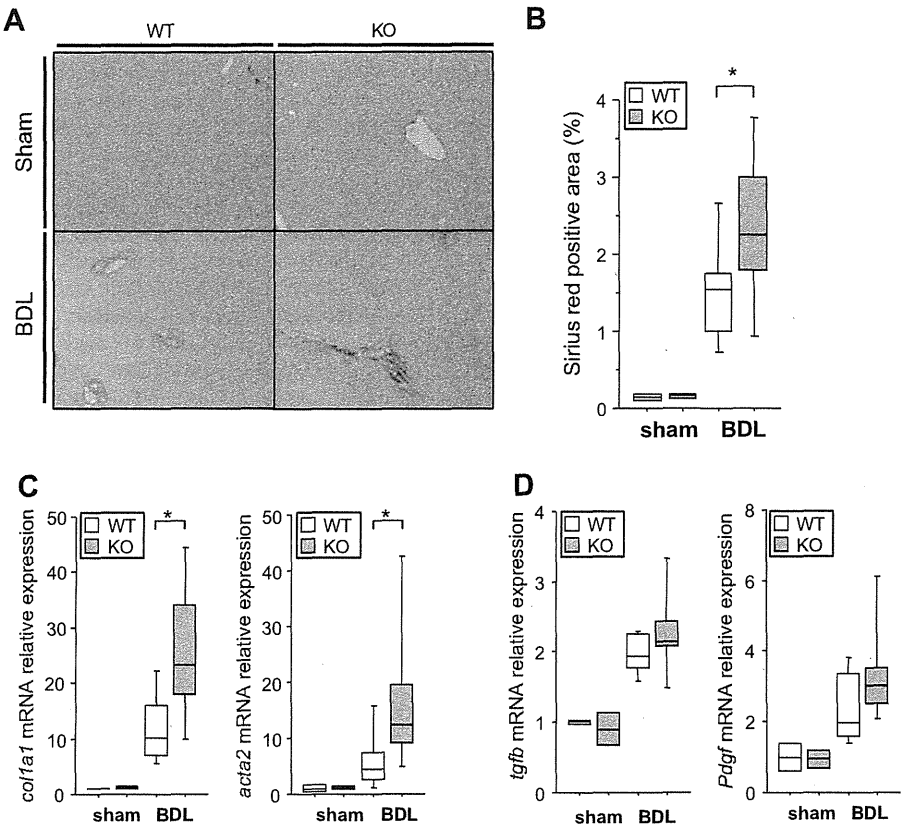

Fig. 2. Exacerbation of liver fibrosis in L-STAT3 KO mice after BDL. L-STAT3 KO mice (KO) and WT littermates (WT) were subjected to BDL or sham-operation (sham) and examined 10 days later. (A) Representative views of picrosirius red staining of the liver sections. (B) Morphometric analysis for picrosirius red staining, $n = 8$/group, $^*p < 0.05$. (C) Hepatic expression of αSMA and type I collagen α1 genes by real-time rtPCR analysis, $n = 8$/group, $^*p < 0.05$. (D) Hepatic expression of TGFβ and PDGF genes by real-time rtPCR analysis, $n = 8$/group.

factors released from hepatocytes repressed activated HSCs and their collagen synthesis. We isolated primary hepatocytes from L-STAT3 KO mice and WT controls, and stimulated them with or without IL-6. The cultured medium of stimulated hepatocytes was collected after 24 h. Whereas faint signals of STAT3 phosphorylation were observed under resting conditions in WT hepatocytes, administration of IL-6 clearly activated STAT3 phosphorylation in WT hepatocytes in contrast to STAT3 KO hepatocytes (Fig. 4A). Accordingly, IL-6 administration activated SAA and haptoglobin gene expression in WT hepatocytes, leading to production of higher levels of SAA and haptoglobin in culture supernatant compared with STAT3 KO hepatocytes (Fig. 4B, Supplementary Fig. 3).

Activated HSCs isolated from C57BL/6J were cultured with supernatant taken from IL-6-treated WT hepatocytes (sup-WT) or that from IL-6-treated STAT3 KO hepatocytes (sup-KO). Activated HSCs were also incubated with medium containing the same amount of IL-6 (sup-control) as a control. The mRNA expression of αSMA and type I collagen α1 in HSCs cultured with sup-WT significantly decreased compared with sup-control (Fig. 4C). On the other hand, the expression of these genes in HSCs cultured with sup-KO was similar to the levels of sup-control (Fig. 4C). In addition, activated HSCs were cultured with recombinant SAA. The expression of αSMA gene in HSCs decreased in dose-dependent manner, although the expression of type I collagen α1 gene did not change (Fig. 4D).

4. Discussion

Liver fibrosis is a consequence of chronic liver injury and inflammation. Accumulating evidence suggests that liver fibrosis is to some extent reversible by appropriate therapeutic intervention for chronic liver diseases [1]. Clarifying the cellular and molecular mechanisms involved in fibrogenesis and its progression has become very important for efficacious treatment. In the present study, we used L-STAT3 KO mice to examine the significance of this signaling pathway in liver fibrogenesis, because hepatocyte STAT3 is a crucial signaling transducer and transcription factor that regulates most, if not all, APPs which have been shown to possess a variety of biological properties during inflammation. We have demonstrated here that lack of STAT3 accelerates liver fibrosis during cholestasis and suggested that STAT3-dependent soluble factors collectively serve as a negative regulator for activation of HSCs.

Very recent research has shown that lack of gp130 or STAT3 in hepatocytes exacerbates liver fibrosis in murine sclerosis cholangitis models induced by 3,5-diethoxycarbonyl-1,4-dihydrocollidine (DDC) diet or genetic deletion of multidrug resistance gene 2 (*mdr2*), respectively. In those studies, deletion of gp130 or STAT3 induced severer cholestasis compared with control mice, leading to enhanced inflammatory cell infiltration and injury in the liver [10,11]. Therefore, exacerbation of liver fibrosis observed in those models might be ascribed to exacerbated cholestasis and liver

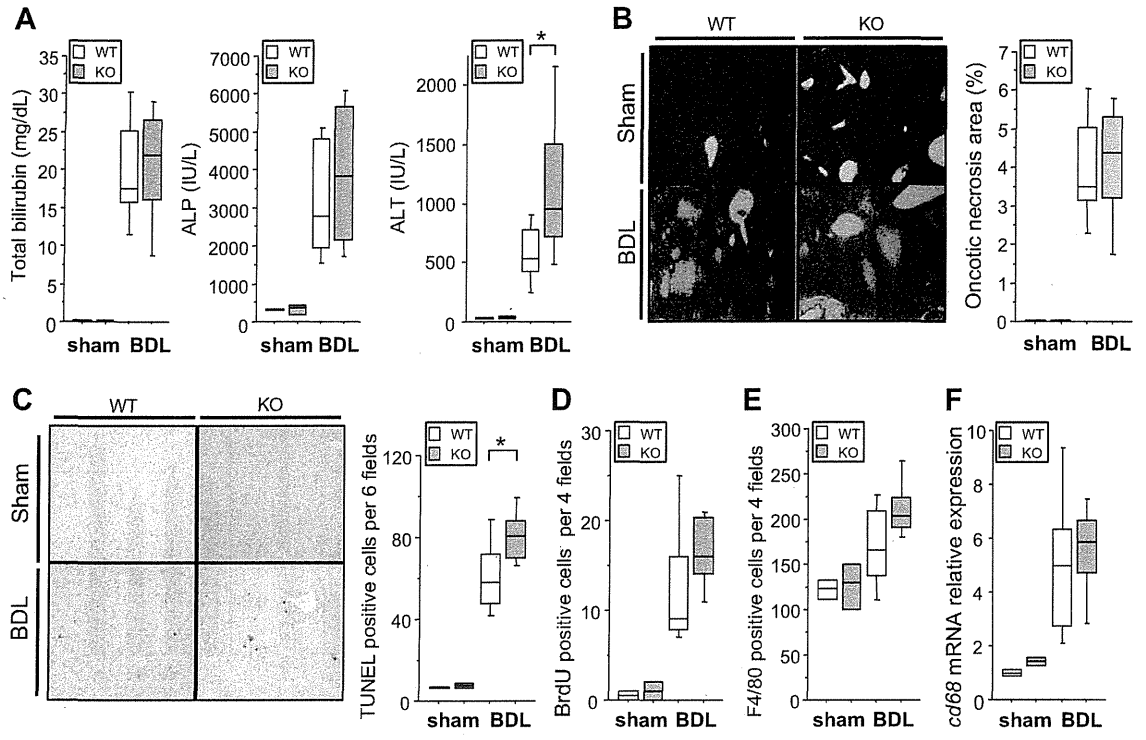

Fig. 3. Exacerbation of liver injury in L-STAT3 KO mice after BDL. L-STAT3 KO mice (KO) and WT littermates (WT) were subjected to BDL or sham-operation (sham) and examined 10 days later. (A) Serum levels of total bilirubin, alkaline phosphatase (ALP) and ALT, $n = 8$/group, $^*p > 0.05$. (B) Representative views of H&E staining of the liver sections and statistics for the area of oncotic necrosis determined by morphometric analysis of H&E staining, $n = 6$/group. (C) Representative views of TUNEL staining of the liver sections and statistics of TUNEL positive cells per 6 fields, $n = 8$/group. (D) The numbers of BrdU-positive cells of the liver sections, $n = 8$/group. 5-bromo-2-deoxyuridine (BrdU) was administered 2 h before sacrifice. (E) The numbers of F4/80-positive cells of the liver sections, $n = 8$/group. The liver sections were stained with anti-F4/80 antigen. (F) Hepatic mRNA expression of CD68 determined by real-time rtPCR analysis, $n = 8$/group.

inflammation. In the present study, we subjected our L-STAT3 KO mice to BDL, a well-established murine model of cholestasis, and examined them 10 days later. We found that hepatocyte-specific deletion of STAT3 promotes liver injury and fibrosis although the mice developed similar levels of cholestasis and inflammatory cell infiltration in the liver, compared with their control littermates. These results clearly indicated that hepatocyte STAT3 signaling negatively regulates liver fibrosis independently of cholestasis and inflammatory cell infiltration in our BDL model. An earlier study showed that deletion of the gp130 gene induced by Cre-mediated recombination under control of the Mx1 gene promoter exacerbated bacterial infection and increased mortality by 10 days after BDL, compared with control mice [17]. In our mice in which STAT3 had been deleted under control of the albumin gene promoter, no rise in mortality occurred after BDL. Since Mx1-Cre-mediated genetic recombination should occur not only in hepatocytes but also in other cell types including a variety of hematopoietic cells, the gp130/STAT3 signaling pathway of other cell types besides hepatocytes might have an impact on the infection control and survival after BDL.

L-STAT3 KO mice showed severer liver injury with increases in the levels of serum ALT and TUNEL-positive cells in the liver sections. This is consistent with the general concept that STAT3 promotes apoptosis resistance by regulating the expression of a variety of anti-apoptotic genes. Indeed previous research showed that the absence of hepatic STAT3 makes hepatocytes more vulnerable to Fas-mediated apoptosis [6]. In contrast to a previous finding that liver regeneration is suppressed in STAT3 KO mice after partial hepatectomy [5], compensatory regeneration after BDL did not differ between L-STAT3 KO mice and the control littermates. Accumulating evidence suggests that hepatocyte apoptosis promotes a liver fibrotic response via HSC activation. Kupffer cells and HSCs were reported to be able to engulf apoptotic bodies and to produce TNFα and TGFβ, respectively [18,19]. These cellular events may lead to the induction of profibrotic responses. Indeed, we previously reported that spontaneous apoptosis did induce mild fibrotic response with increased production of TGFβ *in vivo* [13]. In the present study, STAT3 KO mice displayed increased hepatic expression of αSMA and type I collagen α1 genes suggesting activation of HSCs after BDL, compared with WT controls. However, at the same time, there were no significant differences in the mRNA expression of proinflammatory cytokines such as TNFα (data not shown) and profibrogenic cytokines such as TGFβ and PDGF in the liver between the two groups. This suggested that other factors or cellular events except cytokines or apoptosis were involved in the difference of HSC activation between the two groups in our model.

APPs, defined as proteins whose serum levels change by >25% during inflammation, are mainly produced in the liver and regulated via gp130/STAT3 signaling [20]. Consistent with this, L-STAT3 KO mice showed impaired production of APPs in BDL. Recent research showed that APPs are regarded as important biological components of the immune response to infection and tissue injury [9,21]. The IL-6 family/gp130/STAT3 signaling pathway in hepatocytes regulates the acute phase response and the importance of this pathway during host defense has become evident recently. The present study demonstrated that the absence of STAT3 in hepatocytes during cholestasis led to progression of liver fibrosis as shown by collagen deposition and activation of HSCs. We investigated the direct influence of the soluble factors released from hepatocytes via STAT3 signaling on HSCs activation and collagen production *in vitro*. Interestingly, the mRNA expression of αSMA and type I collagen α1 significantly decreased in activated HSCs

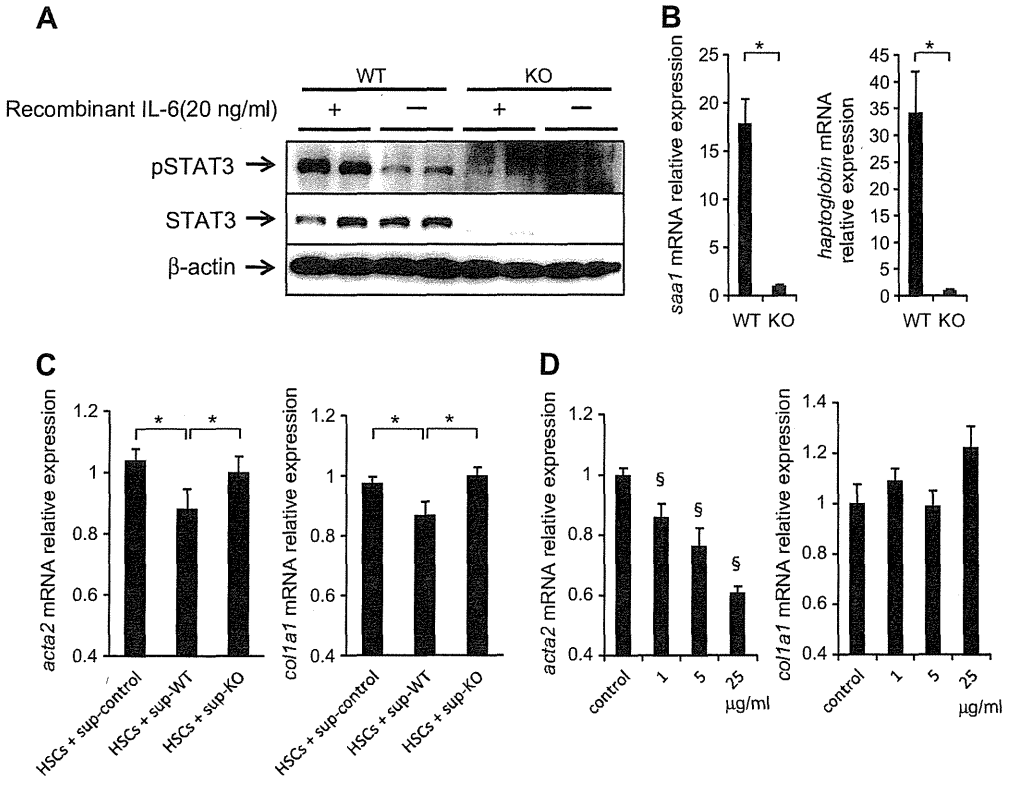

Fig. 4. Involvement of STAT3-dependent hepatic soluble factors in the suppression of activated HSCs. Primary hepatocytes isolated from L-STAT3 KO mice (KO) and WT mice (WT) were stimulated with or without 20 ng/ml of IL-6 for 24 h. (A) Expressions of STAT3 and pSTAT3 in hepatocytes by western blot analysis. β-actin is included as a control. (B) Real-time rtPCR analysis of mRNA expression of SAA and haptoglobin in IL-6-treated hepatocytes, $n = 4$/group, $^{*}p < 0.05$. (C) Real-time rtPCR analysis of αSMA and type I collagen α1 mRNA expression in HSCs, $n = 4$/group, $^{*}p < 0.05$. Activated HSCs were cultured for 24 h with control medium (sup-control), the cultured supernatant from WT hepatocytes (sup-WT) or that from STAT3 KO hepatocytes (sup-KO), stimulated with 20 ng/ml IL-6, respectively. (D) Real-time rtPCR analysis of αSMA and type I collagen α1 mRNA expression in HSCs, $n = 4$/group, $^{§}p < 0.05$ vs the other three groups. Activated HSCs were cultured with recombinant SAA (0, 1, 5, 25 μg/ml) for 24 h.

cultured with sup-WT compared with control medium. In contrast, the expression levels of these genes in activated HSCs remained unchanged when cultured with sup-KO. Since Sup-WT was abundant with SAA and haptoglobin, these findings imply that the hepatocyte STAT3-dependent soluble factors, such as APPs, directly repressed activated HSCs and their collagen production. Indeed, SAA negatively regulated HSC activation, although the mRNA expression of type I collagen α1 was unchanged, providing an example among APPs being able to downregulate activation marker of HSCs. Although further study is needed, the present study suggested that APPs could collectively inhibit HSC activity and collagen production.

In conclusion, the present study demonstrated that the absence of STAT3 in hepatocytes exacerbated liver injury and fibrosis during cholestasis. We speculated that both increase in hepatocyte apoptosis and lack of an acute phase response may contribute to accelerated liver fibrosis in this model. APPs had been individually analyzed to have pro- and anti-inflammatory properties during inflammation. The current study unveiled a previously unrecognized role of STAT3-dependent hepatic APPs in collectively serving as a negative regulator for HSC activation.

Acknowledgments

We thank Dr. S. Akira and Dr. K. Takeda for providing STAT3 floxed mice. This work was supported by a Grant-in-Aid for Scientific Research from the Ministry of Education, Culture, Sports, Science, and Technology, Japan.

Appendix A. Supplementary data

Supplementary data associated with this article can be found, in the online version, at doi:10.1016/j.bbrc.2011.02.105.

References

[1] R. Bataller, D.A. Brenner, Liver fibrosis, J. Clin. Invest. 115 (2005) 209–218.
[2] S. Akira, Y. Nishio, M. Inoue, et al., Molecular cloning of APRF, a novel IFN-stimulated gene factor 3 p91-related transcription factor involved in the gp130-mediated signaling pathway, Cell 77 (1994) 63–71.
[3] T. Taga, T. Kishimoto, Gp130 and the interleukin-6 family of cytokines, Annu. Rev. Immunol. 15 (1997) 797–819.
[4] K. Takeda, K. Noguchi, W. Shi, et al., Targeted disruption of the mouse STAT3 gene leads to early embryonic lethality, Proc. Natl. Acad. Sci. USA 94 (1997) 3801–3804.
[5] W. Li, X. Liang, C. Kellendonk, et al., STAT3 contributes to the mitogenic response of hepatocytes during liver regeneration, J. Biol. Chem. 277 (2002) 28411–28417.
[6] S. Haga, K. Terui, H.Q. Zhang, et al., Stat3 protects against Fas-induced liver injury by redox-dependent and -independent mechanisms, J. Clin. Invest. 112 (2003) 989–998.
[7] H. Inoue, W. Ogawa, M. Ozaki, et al., Role of STAT-3 in regulation of hepatic gluconeogenic genes and carbohydrate metabolism in vivo, Nat. Med. 10 (2004) 168–174.
[8] R. Sakamori, T. Takehara, C. Ohnishi, et al., Signal transducer and activator of transcription 3 signaling within hepatocytes attenuates systemic inflammatory response and lethality in septic mice, Hepatology 46 (2007) 1564–1573.
[9] L.E. Sander, S.D. Sackett, U. Dierssen, et al., Hepatic acute-phase proteins control innate immune responses during infection by promoting myeloid-derived suppressor cell function, J. Exp. Med. 207 (2010) 1453–1464.
[10] W. Plum, D.F. Tschaharganeh, D.C. Kroy, et al., Lack of glycoprotein 130/signal transducer and activator of transcription 3-mediated signaling in hepatocytes

enhances chronic liver injury and fibrosis progression in a model of sclerosing cholangitis, Am. J. Pathol. 176 (2010) 2236–2246.
[11] M. Mair, G. Zollner, D. Schneller, et al., Signal transducer and activator of transcription 3 protects from liver injury and fibrosis in a mouse model of sclerosing cholangitis, Gastroenterology 138 (2010) 2499–2508.
[12] K. Takeda, T. Kaisho, N. Yoshida, et al., Stat3 activation is responsible for IL-6-dependent T cell proliferation through preventing apoptosis: generation and characterization of T cell-specific STAT3-deficient mice, J. Immunol. 161 (1998) 4652–4660.
[13] T. Takehara, T. Tatsumi, T. Suzuki, et al., Hepatocyte-specific disruption of Bcl-xL leads to continuous hepatocyte apoptosis and liver fibrotic responses, Gastroenterology 127 (2004) 1189–1197.
[14] J. Kountouras, B.H. Billing, P.J. Scheuer, Prolonged bile duct obstruction: a new experimental model for cirrhosis in the rat, Br. J. Exp. Pathol. 65 (1984) 305–311.
[15] H. Hikita, T. Takehara, S. Shimizu, et al., The Bcl-xL inhibitor, ABT-737, efficiently induces apoptosis and suppresses growth of hepatoma cells in combination with sorafenib, Hepatology 52 (2010) 1310–1321.
[16] T. Kodama, T. Takehara, H. Hikita, et al., Thrombocytopenia exacerbates cholestasis-induced liver fibrosis in mice, Gastroenterology 138 (2010) 2487–2498.
[17] T. Wuestefeld, C. Klein, K.L. Streetz, et al., Lack of gp130 expression results in more bacterial infection and higher mortality during chronic cholestasis in mice, Hepatology 42 (2005) 1082–1090.
[18] A. Canbay, A.E. Feldstein, H. Higuchi, et al., Kupffer cell engulfment of apoptotic bodies stimulates death ligand and cytokine expression, Hepatology 38 (2003) 1188–1198.
[19] A. Canbay, P. Taimr, N. Torok, et al., Apoptotic body engulfment by a human stellate cell line is profibrogenic, Lab. Invest. 83 (2003) 655–663.
[20] C. Gabay, I. Kushner, Acute-phase proteins and other systemic responses to inflammation, N. Engl. J. Med. 340 (1999) 448–454.
[21] M. Luchtefeld, H. Schunkert, M. Stoll, et al., Signal transducer of inflammation gp130 modulates atherosclerosis in mice and man, J. Exp. Med. 204 (2007) 1935–1944.

Delayed-Onset Caspase-Dependent Massive Hepatocyte Apoptosis upon Fas Activation in Bak/Bax-Deficient Mice

Hayato Hikita,[1]* Tetsuo Takehara,[1]* Takahiro Kodama,[1] Satoshi Shimizu,[1] Minoru Shigekawa,[1] Atsushi Hosui,[1] Takuya Miyagi,[1] Tomohide Tatsumi,[1] Hisashi Ishida,[1] Wei Li,[1] Tatsuya Kanto,[1] Naoki Hiramatsu,[1] Shigeomi Shimizu,[2] Yoshihide Tsujimoto,[3] and Norio Hayashi[4]

The proapoptotic Bcl-2 family proteins Bak and Bax serve as an essential gateway to the mitochondrial pathway of apoptosis. When activated by BH3-only proteins, Bak/Bax triggers mitochondrial outer membrane permeabilization leading to release of cytochrome c followed by activation of initiator and then effector caspases to dismantle the cells. Hepatocytes are generally considered to be type II cells because, upon Fas stimulation, they are reported to require the BH3-only protein Bid to undergo apoptosis. However, the significance of Bak and Bax in the liver is unclear. To address this issue, we generated hepatocyte-specific Bak/Bax double knockout mice and administered Jo2 agonistic anti-Fas antibody or recombinant Fas ligand to them. Fas-induced rapid fulminant hepatocyte apoptosis was partially ameliorated in Bak knockout mice but not in Bax knockout mice, and was completely abolished in double knockout mice 3 hours after Jo2 injection. Importantly, at 6 hours, double knockout mice displayed severe liver injury associated with repression of XIAP, activation of caspase-3/7 and oligonucleosomal DNA breaks in the liver, without evidence of mitochondrial disruption or cytochrome c–dependent caspase-9 activation. This liver injury was not ameliorated in a cyclophilin D knockout background nor by administration of necrostatin-1, but was completely inhibited by administration of a caspase inhibitor after Bid cleavage. Conclusion: Whereas either Bak or Bax is critically required for rapid execution of Fas-mediated massive apoptosis in the liver, delayed onset of mitochondria-independent, caspase-dependent apoptosis develops even in the absence of both. The present study unveils an extrinsic pathway of apoptosis, like that in type I cells, which serves as a backup system even in type II cells. (HEPATOLOGY **2011;54:240-251**)

See Editorial on Page 13

Fas, also called APO-1 and CD95, is one of the death receptors that are potent inducers of apoptosis and constitutively expressed by every cell type in the liver.[1] Dysregulation of Fas-mediated apoptosis is involved in several liver diseases.[2] In the liver of patients with chronic hepatitis C, Fas is overexpressed in correlation with the degree of hepatitis, and Fas ligand can be detected in liver-infiltrating mononuclear cells.[3,4] Fas is also strongly expressed in the livers of patients with chronic hepatitis B, autoimmune hepatitis, and nonalcoholic steatohepatitis.[4,5] Moreover, in the liver of patients with fulminant hepatitis, Fas is up-regulated with strong detection of Fas ligand.[6] In mice, injection of Jo2 agonistic anti-Fas antibody leads

Abbreviations: ALT, alanine aminotransferase; CypD, cyclophilin D; DISC, death-inducing signaling complex; DKO, double knockout; DMSO, dimethylsulfoxide; IAP, inhibition of apoptosis protein; KO, knockout; PARP, poly(adenosine diphosphate ribose) polymerase; RIP, receptor-interacting protein; TUNEL, terminal deoxynucleotidyl transferase–mediated deoxyuridine triphosphate nick-end labeling; WT, wild-type.

From the [1]Departments of Gastroenterology and Hepatology; and [3]Molecular Genetics, Osaka University Graduate School of Medicine, Suita, Osaka, Japan; the [2]Department of Pathological Cell Biology, Medical Research Institute, Tokyo Medical and Dental University, Bunkyo-ku, Tokyo, Japan; and [4]Kansai-Rosai Hospital, Amagasaki, Hyogo, Japan.

Received December 27, 2010; accepted March 9, 2011.

Supported in part by a Grant-in-Aid for Scientific Research from the Ministry of Education, Culture, Sports, Science, and Technology (to T. Takehara) and a Grant-in-Aid for Research on Hepatitis from the Ministry of Health, Labour, and Welfare of Japan.

**These authors contributed equally to this work.*